Research Activities
in
NTT Basic Research Laboratories

Volume 18
Fiscal 2007

July 2008

NTT Basic Research Laboratories,

Nippon Telegraph and Telephone Corporation (NTT)

http://www.brl.ntt.co.jp/

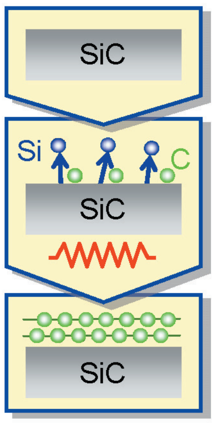

Epitaxial graphene grown on SiC

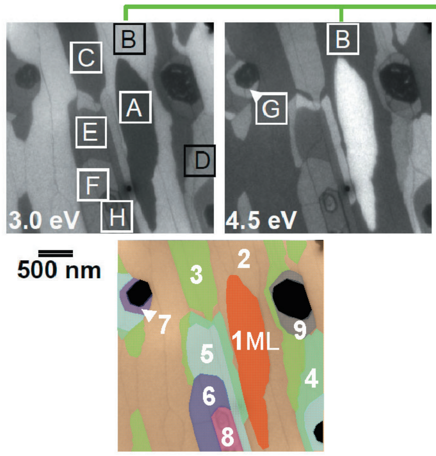

Low-energy electron microscopy images of epitaxial graphene

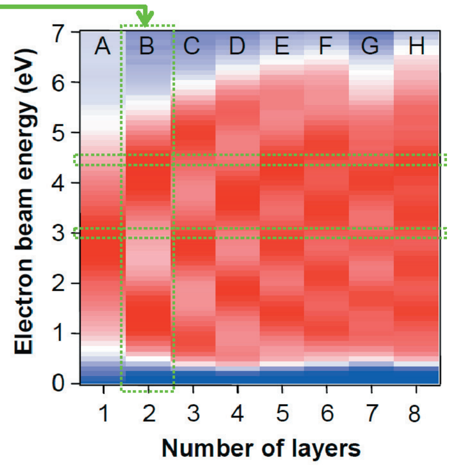

Electron reflectivity map

Evaluation of Number of Graphene Layers Grown on SiC

Recently, graphene has attracted much attention as a material for future electronics. Epitaxial graphene grown on SiC substrates by annealing can be easily scaled up and is promising for device integration. Aiming at establishing a reproducible way of growing large and uniform epitaxial graphene, we demonstrated that the number of graphene layers grown on SiC can be determined by low-energy electron microscopy (LEEM) using quantized oscillations of electron reflectivity. *In-situ* microscopic determination of the number of graphene layers using LEEM would greatly contribute to the growth control of epitaxial graphene. (Page 19)

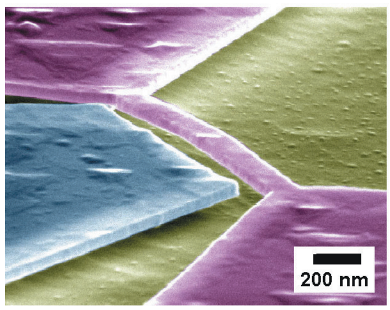

Scanning electron microscopic image of an arched InAs/AlGaSb beam

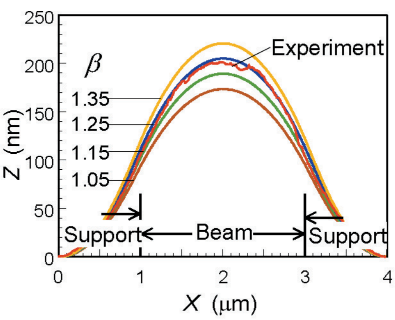

Beam shape measured with an atomic force microscope and calculation results

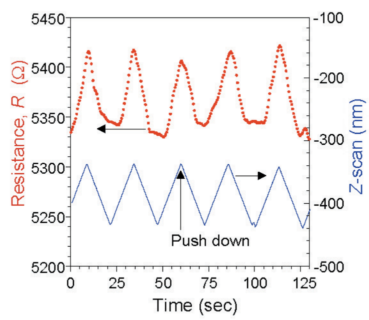

Measurement results: relationship between resistance and beam deflection

Piezoelectric Effect on Piezoresistance of InAs/AlGaSb Heterostructure Nanobeam

Nanoelectromechanical systems comprising compound semiconductors are promising for ultrahigh-sensitivity sensors and other applications. In these systems, piezoresistance (i.e., resistance change due to mechanical strain) is an important parameter. We measured the piezoresistance of InAs/AlGaSb heterostructure nanobeams and found that it strongly depends on whether the beams are arched or straight. This can be explained in calculations of piezoresistance by considering the piezoelectric effect. Our results reveal the importance of the piezoelectric effect in mechanical systems using very thin heterostructures. (Page 26)

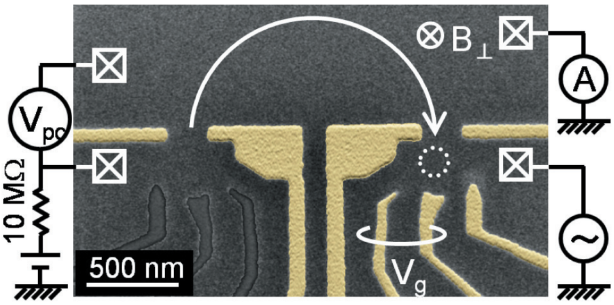

Scanning electron micrograph of device and measurement setup

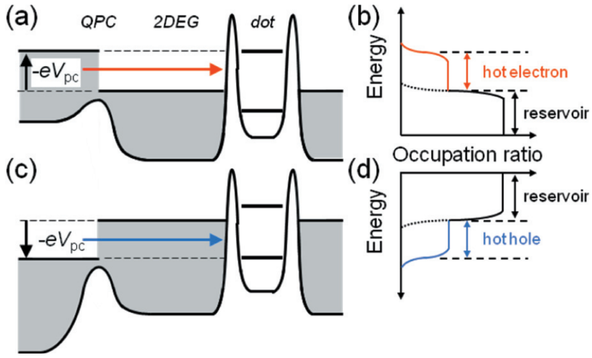

(a,b) Electron accumulation and (c,d) hole accumulation near quantum dot

Energy Distribution Measurement of Nonequilibrium Carriers Using a Quantum Dot

The quantized energy levels of electrons in a semiconductor quantum dot (QD) can be easily tuned by controlling the gate voltage, thus enabling us to use a QD as a high-resolution energy analyzer (or spectrometer) for the electrons near the QD. We used this feature of QDs to measure the energy distribution of ballistic nonequilibrium electrons and holes emitted from a quantum wire. Nonequilibrium carriers were emitted by applying a bias voltage (V_{pc}) to a quantum point contact. The emitted current was again focused by applying a perpendicular magnetic field ($B_{\perp}$) and analyzed with a QD. When the energy of the nonequilibrium carriers coincides with the quantized energy levels, those carriers can resonantly tunnel through the QD and can be detected as an electric current. (Page 31)

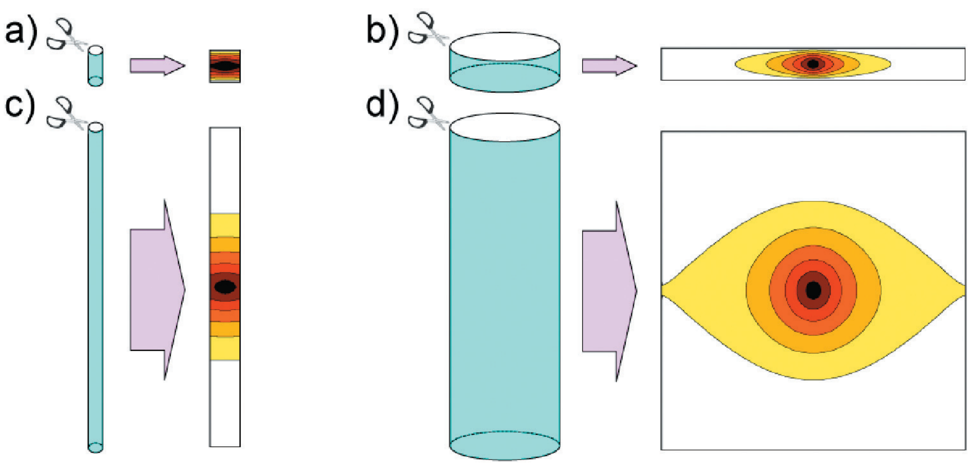

Excitonic wavefunction on four different sized nanotube structures

Topology of Exciton in Artificial Structure

We have theoretically demonstrated that the excitons in nanotube structures show the variety of topological states depending on the size of the nanotube. This is due to the fact that an exciton has its own characteristic size and it determines the confinement feature of the exciton in the structure. It is also shown that the topology of the exciton wavefunction can be controlled through the dielectric constant of the barrier material surrounding the nanotubes. (Page 35)

Message from the Director

We are deeply grateful for your interest and support with respect to our research activities.

The three research areas at NTT-BRL, namely Materials Science, Physical Science, and Optical Science, are undertaking work designed to contribute to the success of NTT's business and promote advances in science that will ultimately benefit all mankind.

A fundamental goal of these research activities is to improve global competitiveness. Therefore, BRL is collaborating with many universities and research institutes throughout the world as well as with other NTT laboratories. BRL organizes international conferences related to quantum physics and also holds a "Science Plaza" to enhance public understanding of our activities and ensure a frank exchange of opinions. Moreover, one of our missions is the education of young researchers and we sponsor the biennial "BRL School", which boasts distinguished researchers as lecturers. In November 2007, thirty-five Ph.D. students and young researchers from universities and institutes in 12 countries participated in the BRL School. We hope that this endeavor will encourage research and contribute to its future growth.

It gives us immense pleasure to fulfill our mission of being an open laboratory in this way, and to disseminate our research output worldwide. Your continued support is greatly appreciated.

Junji Yumoto
Director
NTT Basic Research Laboratories

Contents

page

II. Data

Cover photograph:

Persistent Supercurrent Atom Chip

Atoms in room temperature are moving like a bullet of a handgun, but with a laser cooling technique we can cool them down to one millionth, then the ultra cold atoms start falling down according to gravity. We have succeeded in trapping cold atoms with a practically noise free magnetic potential generated by a persistent current running through a superconducting loop circuit. A silhouette of atoms revealed the fact. A part of this research is supported by the Japan Science and Technology Agency CREST.

Member List

As of March 31, 2008
(* moved to another position within a year)

NTT Basic Research Laboratories

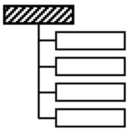

Director, **Dr. Junji Yumoto**

Research Planning Section

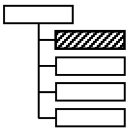

Executive Research Scientist,	**Dr. Toshiki Makimoto** **Dr. Itaru Yokohama***
Senior Research Scientist,	Dr. Hideki Gotoh
Senior Research Scientist, Supervisor,	Dr. Koji Muraki
Senior Research Scientist, Supervisor,	Dr. Yuichi Harada*

NTT R&D Fellow

Prof. Yoshihisa Yamamoto
(Stanford University, U.S.A)
Prof. Hideaki Takayanagi
(Tokyo University of Science)

NTT Research Professor

Prof. Fujio Shimizu
(The University of Electro-Communications)
Prof. Shintaro Nomura
(University of Tsukuba)
Prof. Kyo Inoue
(Osaka University)

Materials Science Laboratory

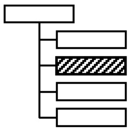

Executive Manager, **Dr. Keiichi Torimitsu**

Assistant Manager, Dr. Hiroo Omi

Dr. Katsuhiro Ajito* Dr. Yuko Ueno*
Dr. Isao Tomita*

Thin-Film Materials Research Group:

Dr. Makoto Kasu (Group Leader)
Dr. Toshiki Makimoto*
Dr. Yasuyuki Kobayashi Dr. Hideki Yamamoto Dr. Hisashi Sato
Dr. Tetsuya Akasaka Dr. Kazuhide Kumakura Dr. Shin-ichi Karimoto*
Dr. Yoshitaka Taniyasu Dr. Kenji Ueda Dr. Atsushi Nishikawa
Dr. Chiun-Lung Tsai Dr. Michal Kubovic

Low-Dimensional Nanomaterials Research Group:

Dr. Yoshihiro Kobayashi (Group Leader)
Dr. Fumihiko Maeda Dr. Hiroki Hibino Dr. Satoru Suzuki
Akio Tokura Dr. Ilya Sychugov

Molecular and Bio Science Research Group:

Dr. Keiichi Torimitsu (Group Leader)
Dr. Keisuke Ebata Dr. Kazuaki Furukawa Dr. Koji Sumitomo
Dr. Nahoko Kasai Dr. Akiyoshi Shimada Dr. Hiroshi Nakashima
Dr. Yoshiaki Kashimura Touichiro Goto Dr. Youichi Shinozaki
Dr. Jonas Rundqvist*

Physical Science Laboratory

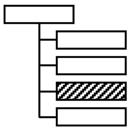

Executive Manager, **Dr. Hiroshi Yamaguchi**

Assistant Manager, Dr. Yukinori Ono

Takeshi Karasawa

Nanodevices Research Group:

Dr. Akira Fujiwara (Group Leader)

Dr. Hiroyuki Kageshima, Dr. Katsuhiko Nishiguchi, Dr.Mohammed Khalafalla

Nanostructure Technology Research Group:

Dr. Hiroshi Yamaguchi (Group Leader)

Dr. Masao Nagase, Dr. Kenji Yamazaki, Toru Yamaguchi, Junzo Hayashi, Dr. Hajime Okamoto, Dr. Koji Onomitsu, Dr. Imran Mahboob, Dr. Vijay Singh

Quantum Solid State Physics Research Group:

Dr. Toshimasa Fujisawa (Group Leader)

Dr. Kiyoshi Kanisawa, Dr. Satoshi Sasaki, Dr. Kyoichi Suzuki, Dr. Toshiaki Hayashi, Dr. Takeshi Ohta, Dr. Norio Kumada, Dr. Kei Takashina, Dr. Paula Giudici*, Dr. Gerardo Gamez, Dr. Kasper Grove-Rasmussen

Superconducting Quantum Physics Research Group:

Dr. Kouichi Semba (Group Leader)

Dr. Hayato Nakano, Dr. Tetsuya Mukai, Dr. Shin-ichi Karimoto, Hirotaka Tanaka, Dr. Shiro Saito, Dr. Kousuke Kakuyanagi, Dr. Ying-Dan Wang, Dr. Yoshiharu Yamada

Spintronics Research Group:

Dr. Tatsushi Akazaki (Group Leader)

Dr. Yuichi Harada, Dr. Hiroyuki Tamura, Dr. Yoshiaki Sekine, Dr. Masumi Yamaguchi, Toshiyuki Kobayashi*, Dr. Hideomi Hashiba

Optical Science Laboratory

Executive Manager, Dr. Yasuhiro Tokura

Assistant Manager, Dr. Atsushi Yokoo

Quantum Optical State Control Research Group:

Dr. Yasuhiro Tokura (Group Leader)

Dr. Kaoru Shimizu	Kazuhiro Igeta	Masami Kumagai
Dr. Makoto Yamashita	Dr. Hiroyuki Shibata	Dr. Hiroki Takesue
Dr. Fumiaki Morikoshi	Dr. Toshimori Honjo	Dr. Kiyoshi Tamaki
Daisuke Hashimoto	Dr. Jens Tobiska*	

Quantum Optical Physics Research Group:

Dr. Hidetoshi Nakano (Group Leader)

Dr. Tetsuomi Sogawa*	Dr. Tadashi Nishikawa	Hidehiko Kamada
Dr. Kouta Tateno	Dr. Takehiko Tawara	Dr. Katsuya Oguri
Dr. Atsushi Ishizawa	Dr. Haruki Sanada	Dr. Guoquiang Zhang

Photonic Nano-Structure Research Group:

Dr. Masaya Notomi (Group Leader)

Dr. Satoki Kawanishi	Dr. Eiichi Kuramochi	Dr. Hideaki Taniyama
Dr. Akihiko Shinya	Dr. Takasumi Tanabe	Dr. Hisashi Sumikura
Dr. Young-Geun Roh*		

Distinguished Technical Members

Toshimasa Fujisawa was born in Tokyo on May 23, 1963. He received the B.E., M.S. and Ph.D. degrees in electrical engineering from Tokyo Institute of Technology in 1986, 1988 and 1991, respectively. He joined NTT Basic Research Laboratories in 1991. He was a guest scientist in Delft University of Technology, Delft, the Netherlands during 1997-1998. Since 2003, he is also a guest associate professor in Tokyo Institute of Technology. Since 1991 he has engaged in the study of semiconductor fine structures fabricated by focused-ion-beam technique and electron-beam lithography technique, transport characteristics of semiconductor quantum dot. His current interests are single-electron dynamics in quantum dots and their application to quantum information technologies. He received Sir Martin Wood Prize in 2003 and JSPS (Japan Society for the Promotion of Science) Award in 2005. He is a member of the Japan Society of Applied Physics, and the Physical Society of Japan.

Masaya Notomi was born in Kumamoto, Japan, on 16 February 1964. He received his B.E., M.E. and Dr. Eng. degrees in applied physics from The University of Tokyo, Japan in 1986, 1988, and 1997, respectively. In 1988, he joined NTT Optoelectronics Laboratories. Since then, his research interest has been to control the optical properties of materials and devices by using artificial nanostructures, and engaged in research on semiconductor quantum wires/dots and photonic crystal structures. He has been in NTT Basic Research Laboratories since 1999, and is currently working on light-propagation control by using various types of photonic crystals. During 1996-1997, he worked for Linköping University in Sweden as a visiting researcher. He is also a guest associate professor in Tokyo Institute of Technology (2003-). He received 2006/2007 IEEE/LEOS Distinguished Lecturer Award. He is a member of the Japan Society of Applied Physics, the American Physical Society, and IEEE/LEOS.

Akira Fujiwara was born in Tokyo, Japan on March 9, 1967. He received his B.S., M.S., and Ph.D. degrees in applied physics from The University of Tokyo, Japan, in 1989, 1991, and 1994, respectively. In 1994, he joined the LSI Laboratories, Nippon Telegraph and Telephone (NTT) Corporation, Kanagawa, Japan. He moved to the Basic Research Laboratories (BRL) in 1996. Since 1994, he has been engaged in research on silicon nanostructures and their application to single-electron devices. He was a guest researcher at the National Institute of Standards and Technology (NIST), Gaithersburg, MD, USA during 2003-2004. He received the SSDM Young Researcher Award in 1998, SSDM Paper Award in 1999, and Japanese Journal of Applied Physics (JJAP) Paper Awards in 2003 and 2006. He was also awarded the Young Scientist Award from the Minister of MEXT (Ministry of Education, Culture, Sports, Science, and Technology) in 2006. He is a member of the Japan Society of Applied Physics and the IEEE.

Advisory Board (2007 Fiscal Year)

Name	Title Affiliation
Gerhard Abstreiter	Professor Walter Schottky Institute Germany
Boris L. Altshuler	Professor Department of Physics Columbia University, U.S.A.
Serge Haroche	Professor Département de Physique De l'Ecole Normale Supérieure, France
Mats Jonson	Professor Department of Physics, Göteborg University, Sweden
Anthony J. Leggett	Professor Department of Physics University of Illinois at Urbana-Champaign, U.S.A.
Johan E. Mooij	Professor Kavli Institute of Nanoscience Delft Delft University of Technology, The Netherlands
John F. Ryan	Professor Clarendon Laboratory University of Oxford, U.K.
Klaus von Klitzing	Professor Max-Planck-Institut für Festkörperforschung Germany

Invited / Guest Scientists (2007 Fiscal Year)

Name	Title Affiliation
Dr. Go Yusa	Japan Science and Technology Agency (JST), Japan October 05 ~
Assoc. Prof. Shin-ichi Warisawa	The University of Tokyo, Japan May 07 – March 08
Dr. Kasper Grove-Rasmussen	University of Copenhagen, Denmark July 07
Assoc. Prof. Taka-aki Koga	Hokkaido University, Japan November 06 ~
Dr. Akira Yamazaki	Meiji University, Japan November 06 – March 08
Dr. Alexandre Kemp	Japan Science and Technology Agency (JST), Japan December 06 – March 08
Dr. Hongwu Liu	Japan Science and Technology Agency (JST), Japan February 07 – March 08
Dr. Chandra Ramanujan	University of Oxford, U.K. April 07
Dr. Takashi Uchida	Japan Science and Technology Agency (JST), Japan April 07 – March 08
Dr. Qiang Zhang	Stanford University, U.S.A. June 07 – July 07
Prof. Shmuel Gurvitz	Weizmann Institute, Israel July 07 – September 07
Assoc. Prof. Hongxiang Li	Chinese Academy of Sciences, China August 07 – October 07
Dr. Na Young Kim	Stanford University, U.S.A. November 07 – December 07
Dr. Keiko Kato	National Institute for Materials Science (NIMS), Japan December 07 – June 08

Overseas Trainees (2007 Fiscal Year)

Name	Affiliation	Period
Simon Perraud	University of Paris 6 / CNRS, France	Oct. 04 – Sep. 07
Christoph Hufnagel	University of Heidelberg, Germany	June 06 – June 07
Michailas Romanovas	Vilnius Gediminas Technical University, Lithuania	Jan. 07 – Aug. 07
Joana Durao	University of Porto, Portugal	Jan. 07 – Aug. 07
Ari Siitonen	University of Kuopio, Finland	Jan. 07 – Aug. 07
Daan Sprunken	University of Twente, The Netherlands	Jan. 07 – Aug. 07
Sylvain Sergent	INSA (Institut National des Sciences Appliquées de Rennes), France	Jan. 07 – Aug. 07
Florian Domengie	INSA (Institut National des Sciences Appliquées de Toulouse), France	Feb. 07 – Sep. 07
Guillaume Vincent	INSA (Institut National des Sciences Appliquées de Toulouse), France	Feb. 07 – Sep. 07
Yosia	Nanyang Technological University, Singapore	Apr. 07 – Apr. 08
Marcus Eichfelder	Institut für Halbleiteroptik und Funktionelle Grenzflächen, Germany	June 07 – Oct. 07
Stephane Salib	ESPCI (Ecole Superieure de Physique et de Chimie Industrielle), France	July 07 – Aug. 07
Akira Matsudaira	University of Illinois at Urbana-Champaign, U.S.A.	May 07 – July 07
Matthieu Delbecq	ESPCI (Ecole Superieure de Physique et de Chimie Industrielle), France	July 07 – Dec. 07
Charlie Koechlin	ESPCI (Ecole Superieure de Physique et de Chimie Industrielle), France	July 07 – Dec. 07
Edita Kirpsaite	Kaunas University of Technology, Lithuania	Jan. 08 – Aug. 08
Miron Sadziak	Warsaw University, Poland	Jan. 08 – Aug. 08
John McGurk	Imperial College London, U.K.	Jan. 08 – Aug. 08
Zhenzhong Wang	Chinese Academy of Sciences, R.O.C.	Jan. 08 – Dec. 08
Thibaut Balois	Ecole Normale Supérieure, France	Feb. 08 – July 08
Thomas Panier	Ecole Normale Supérieure, France	Feb. 08 – July 08
Benjamin Miquel	Ecole Normale Supérieure, France	Feb. 08 – July 08
Justin Pinkney	University of Oxford, U.K.	Feb. 08 – Mar. 08
Paul Köcher	University of Oxford, U.K.	Feb. 08 – Mar. 08

Domestic Trainees (2007 Fiscal Year)

Name	Affiliation	period
Yuichi Igarashi	The University of Tokyo	Apr. 07 – Mar. 08
Daisuke Itoh	Tohoku University	Apr. 07 – Mar. 08
Shoko Utsunomiya	The University of Tokyo	Apr. 07 – Mar. 08
Taichi Urayama	Keio University	Apr. 07 – Mar. 08
Akira Oiwa	The University of Tokyo, Lecturer	Apr. 07 – Mar. 08
Minoru Oda	The University of Tokyo	Apr. 07 – Mar. 08
Seiichiro Kagei	Tokyo University of Science	Apr. 07 – Mar. 08
Ryo Kajiura	Tokyo Institute of Technology	Apr. 07 – Mar. 08
Keiichi Katoh	The University of Tokyo	Apr. 07 – Mar. 08
Takayuki Kaneko	Meiji University	Apr. 07 – Mar. 08
Takehito Kamada	Tohoku University	Apr. 07 – Mar. 08
Ken-ichiro Kusudo	The University of Tokyo	Apr. 07 – Mar. 08
Takashi Kobayashi	Tohoku University	Apr. 07 – Mar. 08
Jonathan Baugh	The University of Tokyo, Visiting researcher	Apr. 07 – Aug. 07
Go Shinkai	Tokyo Institute of Technology	Apr. 07 – Mar. 08
Masaya Tazawa	Tokyo University of Science	Apr. 07 – Mar. 08
Koujiro Tamaru	The University of Tokyo	Apr. 07 – Mar. 08
Shun Chikamori	Tokyo Institute of Technology	Apr. 07 – Mar. 08
Shouei Tsuruta	Tokyo University of Science	Apr. 07 – Mar. 08
Eigo Totoki	The University of Tokyo	Apr. 07 – Mar. 08
Keiichiro Nonaka	The University of Tokyo	Apr. 07 – Mar. 08
Takuro Hashimoto	Shibaura Institute of Technology	Apr. 07 – Mar. 08
Ken-ichi Hidachi	The University of Tokyo	Apr. 07 – Mar. 08
Hirotaka Masuyama	Tokyo University of Science	Apr. 07 – Mar. 08
Takao Yamaguchi	Tokai University	Apr. 07 – Mar. 08
Mizuki Miyamoto	Shonan Institute of Technology	Apr. 07 – Mar. 08
Shin Yabuuchi	Keio University	Apr. 07 – Mar. 08
Michihisa Yamamoto	The University of Tokyo, Assistant	Apr. 07 – Mar. 08
Hiroshi Kamata	Tokyo Institute of Technology	Apr. 07 – Mar. 08
Hiroki Nose	Tokyo Institute of Technology	Apr. 07 – Mar. 08
Yuki Ichigo	Tokyo University of Science	Apr. 07 – Mar. 08
Hiroyuki Suzuki	Tokyo Institute of Technology	Apr. 07 – Mar. 08

Name	Affiliation	Period
Ryota Koibuchi	Tokyo University of Science	May 07 – Mar. 08
Satoru Miyamoto	Keio University	May 07 – Mar. 08
Keita Kimura	The University of Tokyo	May 07 – Mar. 08
Shun Takahashi	The University of Tokyo	May 07 – Mar. 08
Sangyoon Lee	The University of Tokyo	May 07 – Mar. 08
Hiroki Morishita	Keio University	May 07 – Mar. 08
Takayuki Yamamoto	The University of Tokyo	June 07 – Mar. 08
Tomoyuki Mizuno	Keio University	June 07 – Mar. 08
Yasuno Ozaki	The University of Tokyo	June 07 – Jan. 08
Yasutaka Nakai	The University of Tokyo	June 07 – Mar. 08
Yuji Sakai	Tokyo University of Science	June 07 – Mar. 08
Kenji Yamaya	Tokyo University of Science	June 07 – Mar. 08
Yasuaki Miyazaki	Keio University	June 07 – Mar. 08
Naoyuki Masumoto	The University of Tokyo	July 07 – Mar. 08
Yuma Okazaki	Tohoku University	Aug. 07 – Mar. 08
Lei Zhu	The University of Tokyo	Aug. 07 – Aug. 07
Ichiro Yamato	The University of Tokyo	Aug. 07 – Aug. 07
Yoshitaka Niida	Tohoku University	Aug. 07 – Mar. 08
Yuki Iwai	Osaka University	Sep. 07 – Mar. 08
Norihito Hibino	Keio University	Oct. 07 – Mar. 08
Kazuya Saginawa	Nagaoka University of Technology	Oct. 07 – Feb. 08
Kuniaki Yamada	Keio University	Nov. 07 – Mar. 08
Yoshiaki Ogasawara	Kyoto University	Nov. 07 – Dec. 07
Takenori Matsumoto	Tokai University	Dec. 07 – Feb. 08
Eiji Ueno	Tokai University	Dec. 07 – Feb. 08
Junichi Sato	Tokai University	Dec. 07 – Feb. 08
Monica Craciun	The University of Tokyo, Postdoc	Dec. 07 – Mar. 08
Saverio Russo	The University of Tokyo, Postdoc	Dec. 07 – Mar. 08
Hiroshi Takahashi	Tokyo Institute of Technology	Dec. 07 – Mar. 08
Kouhei Hatafuku	Toyohashi University of Technology	Jan. 07 – Feb. 08
Atsushi Yamamoto	Osaka University	Feb. 08 – Mar. 08
Akira Wada	Tohoku University	Feb. 08 – Mar. 08

Ⅰ. Research Topics

Overview of Research in Laboratories

Material Science Laboratory

Keiichi Torimitsu

The Materials Science Laboratory aims at producing new functional materials and designing of advanced device based on novel materials and biological function. Controlling the configuration and coupling of atoms and molecules is our approach to accomplish these goals. Bio-nano research and diamond-device research are set as the principle research in our laboratory.

We have three research groups covering from semiconductor devices, such as GaN, to organic materials, such as receptor proteins. The characteristic feature of our laboratory is the effective sharing of the unique materials and measurement techniques of each group. This enables fusion of research fields and techniques, which leads to innovative material research for the IT society.

We set up European laboratory in U.K. for bio-nano research, our principal research, in October 2004 and strengthen our research activities. We promote collaborations with international organizations to develop a firm basis of basic science.

Physical Science Laboratory

Hiroshi Yamaguchi

We are studying semiconductor and superconductor-based solid-state devices, which will have a revolutionary impact on communication and information technologies in the 21st century. In particular, we promote research of nanoscale devices fabricated using high-quality crystal growth and fine lithographic techniques.

The five groups in our laboratory are working in the following areas: precise and dynamical control of single electrons, nanodevices operating with ultra low power consumption, novel nanomechanical systems utilizing mechanical degrees of freedom in solid-state architechtures, coherent quantum control of semiconductor and superconductor systems, carrier interactions in semiconductor hetero- and nanostructures, atom chips, spintronics manipulating both electron and nuclear spins. We also promote the studies of cutting-edge nanolithography techniques, high-quality crystal growth, and theoretical studies including first-principle calculations.

Optical Science Laboratory

Yasuhiro Tokura

This laboratory aims for the development of core-technologies that will innovate on optical communications and optical signal processing, and seeks fundamental scientific progresses.

The groups in our laboratory are working for the quantum state control by very weak light, the search for intriguing phenomena using very intensive and short pulse light, and very small optical integrated circuits using two-dimensional photonic crystals, based on the optical properties of semiconductor nanostructures like a quantum dot.

In this year, we realized improvements of quantum cryptography using entangled photon pairs, optical properties of high quality semiconductor nanowires, and a coupled resonator waveguide formed by ultrahigh-Q photonic crystal nano-resonators.

Polarized Emission of AlN Deep-UV LED by a Negative Crystal-field Splitting Energy

Yoshitaka Taniyasu and Makoto Kasu
Materials Science Laboratory

Aluminum nitride (AlN) is a direct-bandgap semiconductor with a bandgap energy of 6 eV, the largest among semiconductors, and is therefore promising for light-emitting devices with the shortest wavelength. We have succeeded in p-type and n-type doping of AlN and have fabricated an AlN light-emitting diode (LED). In this study, to gain insight into the light emission mechanism, we characterized the radiation properties.

An AlN LED was grown on SiC (0001) substrate by metalorganic vapor phase epitaxy. Figure 1 shows the radiation properties of the AlN LED. The radiation angle θ is defined as the angle from the surface normal (c-axis direction) to the detection direction. As the radiation angle increases, the intensity of the near-band-edge emission at 210 nm increases. To clarify the reason, we analyzed the relationship between the emission intensity and the radiation angle as shown in Fig. 2. Solid lines are calculated results for different polarization ratios P. P = 1 corresponds to polarized light parallel to the c-axis (E||c), P = −1 corresponds to polarized light perpendicular to the c-axis (E⊥c), and P = 0 corresponds to unpolarized light. The experimental values follow the calculated one for P = 0.995. This indicates that the emission strongly polarizes for E||c. As a result, the emission intensity has the maximum perpendicular to the c-axis and the minimum parallel to it. Therefore, as the radiation angle increases from the c-axis, the emission intensity increases as shown in Fig. 1 [1].

The origin of the strong polarization can be explained by the band structure. Because AlN has strong ionicity, the lattice is strongly distorted. As a result, the crystal-field splitting energy has a negative value and the top valence band therefore becomes the Γ_{7V} band. A transition between the top valence band Γ_{7V} and conduction band Γ_{7C} is allowed for E||c but is almost completely prohibited for E⊥c. Therefore, the near-band-edge emission strongly polarizes for E||c. Using a crystal-field splitting energy Δ_{CRY} = –230 meV and a spin orbital splitting energy Δ_{SO} = 20 meV, P was calculated to be 0.997, which is in good agreement with the experimentally obtained value. Thus, we found that the strong polarization results from the negative crystal-field splitting energy.

This work was partly supported by Grant-in-Aid for Young Scientists (A), 19686003, from the Ministry of Education, Culture, Sports, Science and Technology, Japan.

[1] Y. Taniyasu, M. Kasu, and T. Makimoto, Appl. Phys. Lett. **90** (2007) 261911.

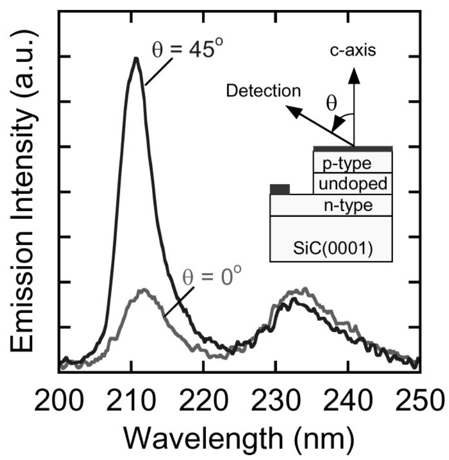

Fig. 1. Radiation properties of AlN LED.

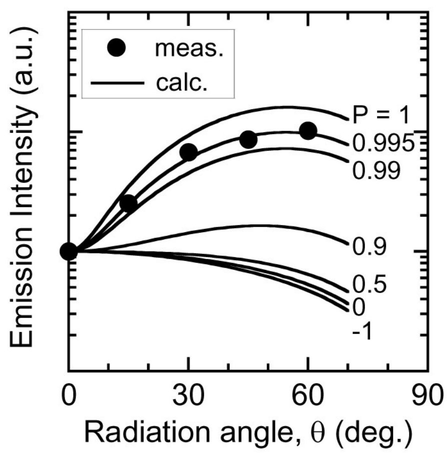

Fig. 2. Light emission intensity as a function of radiation angle.

Doping of Diamond by Combining Ion-implantation and High-pressure and High-temperature Annealing

Kenji Ueda and Makoto Kasu
Materials Science Laboratory

Ion implantation is a widely used doping technique for semiconductors such as Si and GaAs. However, ion implantation severely damages the crystal. In Si and GaAs, the damage can be easily recovered by thermal annealing in a vacuum or in an inert gas. However, it is extremely difficult to recover the damage in diamond by thermal annealing. One possible reason is that the annealing condition is not located in diamond's stable region but rather in graphite's stable region. Therefore, we propose high-pressure and high-temperature (HPHT) annealing as a new activation method for ion-implanted dopants in diamond. The concept is to recover from implantation-induced damage by annealing under high pressure, that is, under diamond's stable condition (Fig. 1) [1, 2]. Here, we show that HPHT annealing is highly effective for damage recovery in ion-implanted diamond.

Homoepitaxial diamond films were grown on Ib-type diamond (100) single crystals by microwave plasma CVD. Boron (B) ions were implanted at an acceleration voltage of 60 keV with a dose of 1×10^{15} cm^{-2}. The HPHT annealing of the B-implanted films was performed using a cubic-anvil-type high-pressure apparatus. The pressure was fixed at ~7 GPa and the annealing temperature was changed from 1200 to 1400 ^{o}C. Thermal annealing of the B-implanted films was also performed in a vacuum for comparison.

Figure 2 compares the annealing temperature (T_a) dependence of doping efficiency of the B-implanted films after HPHT annealing and conventional thermal annealing evaluated from Hall measurements. The doping efficiency of HPHT-annealed films increased exponentially as T_a increased and reached 7.1 % at 1400 ^{o}C. In contrast, the doping efficiency for conventional thermal annealing increased linearly and reached 0.73 % at 1400 ^{o}C. At the same T_a of 1400 ^{o}C, the doping efficiency for HPHT-annealed films is 10 times higher than that for conventional thermal annealing. These results indicate HPHT annealing is much more effective for activation of ion-implanted dopants than conventional thermal annealing.

This work was partly supported by the SCOPE project of the Ministry of Internal Affairs and Communications, Japan.

[1] K. Ueda, M. Kasu, A. Tallaire, and T. Makimoto, Diamond Relat. Mater. **15** (2006) 1789.
[2] K. Ueda, M. Kasu, and T. Makimoto, Appl. Phys. Lett. **90** (2007) 122102.

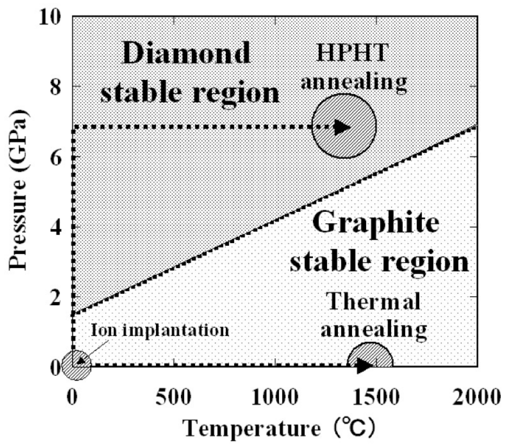

Fig. 1. Phase diagram of carbon, which shows conditions for HPHT annealing and conventional thermal annealing.

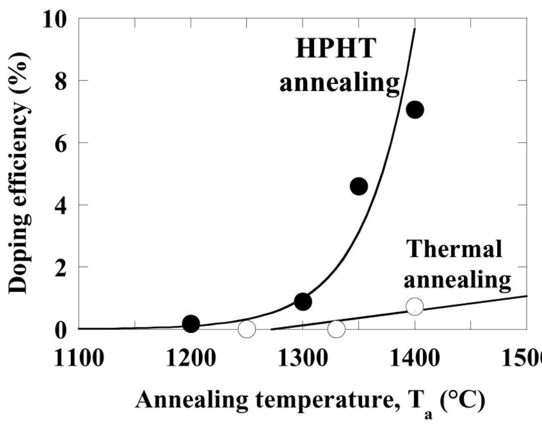

Fig. 2. Doping efficiency of the B-implanted films after HPHT annealing and conventional thermal annealing.

Quasi Two-dimensional Hole Channel in Diamond FETs

Makoto Kasu and Kenji Ueda
Materials Science Laboratory

Diamond is expected to exhibit the best performance as an RF power transistor because it has the highest breakdown field strength and thermal conductivity and relatively high mobility and saturation velocity. Recently, we have reported high RF performance in diamond FETs using H surface-termination as p-type doping: cut-off frequencies of the current gain, f_T (transition frequency), of 45 GHz and of the power gain, f_{MAX} (maximum frequency of oscillation), of 120 GHz, and RF output power density of 2.1 W/mm at 1 GHz in class-A operation. These values are the highest among diamond at present and high enough for power amplifiers in wireless base stations. However, the mechanism of H surface-termination in diamond FETs is still controversial, and the band diagram of a diamond FET has not been clarified yet.

We have extracted the gate voltage dependence V_{GS} of RF transconductance g_m and gate-source capacitance C_{GS} from S-parameter measurements of an FET with gate length (L_G) of 0.1 μm and gate width (W_G) of 50 μm, as shown in Fig. 1 [1]. The most significant finding is that C_{GS} shows a plateau for -0.5 V < V_{GS} < -2.0 V. In the FET fabrication process, Al gate metal was deposited directly on H-terminated diamond surface. However, this characteristic unambiguously indicates that an energy barrier forms between the gate metal and two-dimensional hole channel and that the diamond FET functions as a MISFET. We have proposed the energy band diagram of the diamond FET, as shown in Fig. 2.

As shown in Fig. 1, for V_{GS} > -0.5 V, as positive V_{GS} increases, g_m decreases and C_{GS} decreases. This means that as positive V_{GS} increases, the depletion layer below the energy barrier extends to the substrate side (Fig. 2). For V_{GS} < -2.0 V, as negative V_{GS} increases, g_m decreases and at the same time C_{GS} increases steeply. This characteristic indicates that the energy barrier becomes a triangular potential barrier and then holes penetrate the energy barrier, and consequently C_{GS} increases. In Fig. 1, the C_{GS} value at the plateau is 0.037 pF and its capacitance normalized by the gate area is estimated to be 0.74 μF/cm^2. Assuming the dielectric constant of diamond and Al_2O_3, the interfacial-layer thickness is estimated to be 7~10 nm. By cross-sectional TEM observation, we have confirmed a 7~10 nm-thick interfacial layer between Al gate metal and H-terminated diamond [2].

This work was partly supported by the SCOPE project, "Diamond RF Power Amplifiers", from the Ministry of Internal Affairs and Communications, Japan.

[1] M. Kasu, et al., Appl. Phys. Lett. **90** (2007) 043509.
[2] M. Kasu, et al., Diamond and Relat. Mater. **17** (2008) in press.

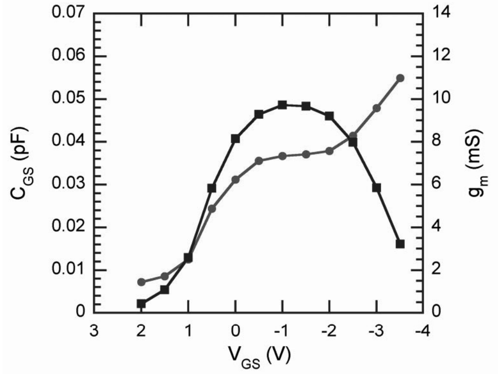

Fig. 1. Gate voltage dependence of gate capacitance and transconductance.

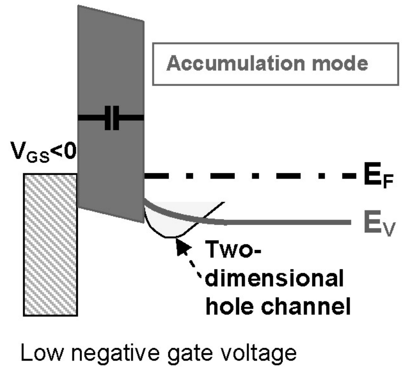

Fig. 2. Proposed band diagram of the diamond FET.

High-temperature Characteristics of *npn*-type GaN/InGaN Double Heterojunction Bipolar Transistors

Atsushi Nishikawa, Kazuhide Kumakura, and Toshiki Makimoto
Materials Science Laboratory

GaN-based electronic devices are expected to be advantageous for high-power and high-temperature operation compared with conventional GaAs- or Si-based devices because of the wide band gap of GaN. In the previous studies, we have succeeded in obtaining the high current gain of over 2000 [1] and high-power characteristics of 270 kW/cm^2 [2] for the *npn*-type GaN/InGaN double heterojunction bipolar transistors (DHBTs). Our next target is to demonstrate the high-temperature operation of these DHBTs. In this study, we investigated the temperature dependence of the common-emitter current-voltage (*I-V*) characteristics of *npn*-type GaN/InGaN DHBTs [3].

GaN/InGaN DHBT structures were grown on SiC substrates using low-pressure metal-organic vapor phase epitaxy. The sample structure consisted of a 40-nm-thick *n*-GaN emitter, a 100-nm-thick *p*-InGaN base, a 30-nm-thick graded InGaN layer, a 500-nm-thick *n*-GaN collector, a 1-μm-thick *n*-GaN sub-collector, and an AlN buffer layer. The In composition of *p*-InGaN base was 7%. The emitter size was 50 × 30 μm^2.

Figure 1 shows the common-emitter *I-V* characteristics of the GaN/InGaN DHBT measured at 300 °C. The base current is 50 μA/step. Even though the current gain ($\beta = \Delta I_C/\Delta I_B$) decreases with increasing temperature, the maximum current gain at 300 °C is still as high as 308. The maximum current density at 300 °C is calculated to be as high as 5.5 kA/cm^2. As shown in Fig. 2, the temperature dependence of the maximum current gain of the GaN/InGaN DHBT follows an exponential dependence with activation energy of 0.13 eV. Since the activation energy of the reduction of the current gain is larger than the expected value assuming the increase in the hole back-injection current from the base into the emitter (0.06 eV), an increase in the carrier concentration of the *p*-$In_{0.07}Ga_{0.93}N$ base, which activation energy is 0.12 eV, is considered to be attributed to the reduction of the current gain.

[1] T. Makimoto, K. Kumakura, and N. Kobayashi, Appl. Phys. Lett. **83** (2003) 1035.
[2] T. Makimoto, Y. Yamauchi, and K. Kumakura, Appl. Phys. Lett. **83** (2004) 1964.
[3] A. Nishikawa, K. Kumakura, and T. Makimoto, Appl. Phys. Lett. **91** (2007) 133514.

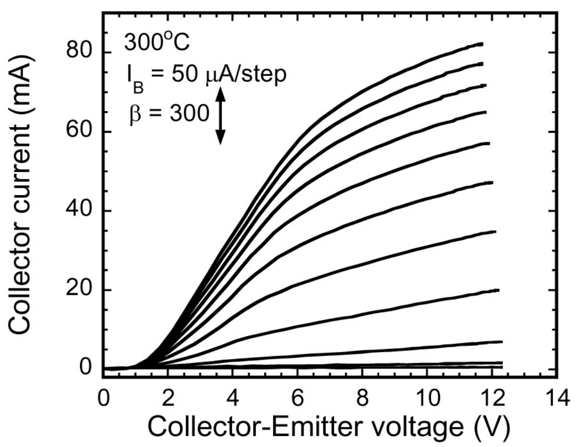

Fig. 1. Common-emitter *I-V* characteristics measured at 300 °C.

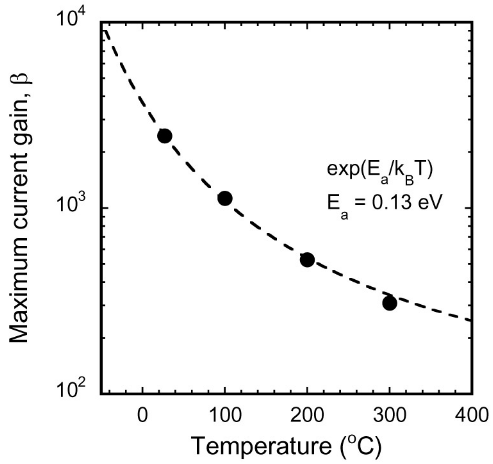

Fig. 2. Temperature dependence of the maximum current gain of GaN/InGaN DHBT.

Raman Spectroscopy of Carbon Nanotubes at CVD Growth Temperature and the Assignments of their Chiral Indices

Takashi Uchida and Yoshihiro Kobayashi
Materials Science Laboratory

Whether we will be successful in applying carbon nanotubes (CNTs) to electronic devices highly depends on our ability to synthesize CNTs with a desired chirality, because the electronic structures of CNTs strongly depends on their chirality. To control the growth of CNTs, it is important to clarify their growth mechanism. We have investigated CVD growth processes of CNTs by *in-situ* Raman observation. Raman spectra are strongly temperature-dependent because they reflect the vibrational properties of observed materials. In order to discuss the details of the growth process observed by *in-situ* Raman spectroscopy, temperature effects in the Raman spectra of CNTs should be elucidated.

Figure 1 shows an atomic force microscope (AFM) image of a CNT-grown sample. Individual CNTs lie on the substrate. Figure 2 shows (a) the experimental Kataura plot and (b) RBM signals observed at 720 ^{o}C (during CVD) and at room temperature (after CVD). The chiral indices of the RBM signals observed at room temperature can be assigned as shown in Fig. 2(b) on the basis of the experimental Kataura plot. The RBM peak frequencies tend to simply decrease with increasing temperature. This is a commonly observed phenomenon originating from the softening of the force constant with increasing temperature. In addition, the relative intensities of each RBM peak change with temperature. This temperature dependence is explained by the change in the resonance condition of each RBM peak. The optical transition energy of nanotubes decreases with increasing temperature, resulting in a shift of each point in the Kataura plot to the lower left as shown in Fig. 2(a). From this analysis, the chiral indices of the RBM peaks observed at CVD growth temperature of 720 ^{o}C are successfully assigned as shown in Fig. 2(b) [1]. These results encourage us to further investigation of the chirality-dependent growth behavior of CNTs observed with *in-situ* Raman spectroscopy and, in future, will lead us to clarifying growth mechanism and thereby achieve the chirality-controlled growth of CNTs.

[1] T. Uchida, et al., Appl. Surf. Sci., in press.

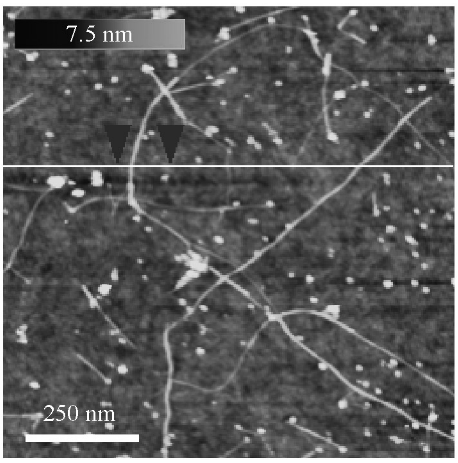

Fig. 1. AFM image of the CNT sample.

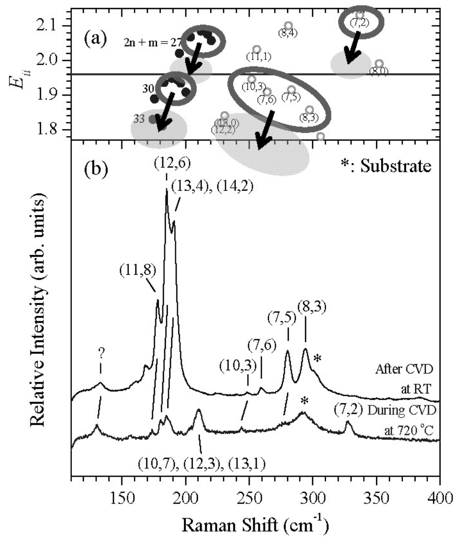

Fig. 2. (a) Experimental Kataura plot: RBM frequencies ω_{RBM} vs the optical transition energies E_{ii}. (b) RBM signals observed during CVD at 720 ^{o}C and after CVD at 25 ^{o}C.

Low-Energy Irradiation Damage in Carbon Nanotubes

Satoru Suzuki and Yoshihiro Kobayashi
Materials Science Laboratory

Single-walled carbon nanotubes (SWNTs) are promising material as a constituent of future nano-electronics because of their nanometer-scale diameter and excellent electric, chemical, and mechanical properties. We have reported that SWNTs are damaged by low-energy electron and photon irradiation and that their electric properties are largely altered from metallic to semiconducting, or even to insulating, by moderate damage [1]. Recently, we have found that defects induced by low-energy irradiation have some unique characteristics.

In the case of knock-on damage caused by high-energy particle irradiation, the SWNTs can not be fully recovered by annealing because ejected atoms are lost. On the other hand, one of important properties of low-energy irradiation damage is that the SWNTs can recover [2]. Raman spectra (radial breathing mode [RBM] region) of pristine, irradiated, and annealed SWNTs are shown in Fig. 1. The RBM frequency depends on the diameter, and thinner nanotubes have larger frequencies. All of the RBM peaks disappeared except for that of the thickest SWNTs, but they reappeared after annealing. This indicates that the number of carbon atoms remains constant with defect formation. Our results also reveal that the damage and recovery strongly depends on the diameter: that is, thinner SWNTs are more easily damaged and hardly recover (see Fig. 1). Moreover, the damaged SWNTs were found to recover even at room temperature or below. The activation energy of the defect healing was estimated to be about 1 eV (depending on the diameter) by observing recovery process by means of electric conductivity [3]. Whereas, the threshold energy of defect formation was determined to be about 6 eV from the results of monochromated vacuum ultra-violet light irradiation experiments. The energetics of the defect formation and healing is summarized in Fig. 2. We will try to determine the detailed atomic structure of the defects and to control the device performance by defect engineering.

[1] A. Vijayaraghavan, et al., Nano Lett. **5** (2005) 1575.
[2] S. Suzuki and Y. Kobayashi, Chem. Phys. Lett. **430** (2006) 370.
[3] S. Suzuki and Y. Kobayashi, J. Phys. Chem. C **111** (2007) 4524.

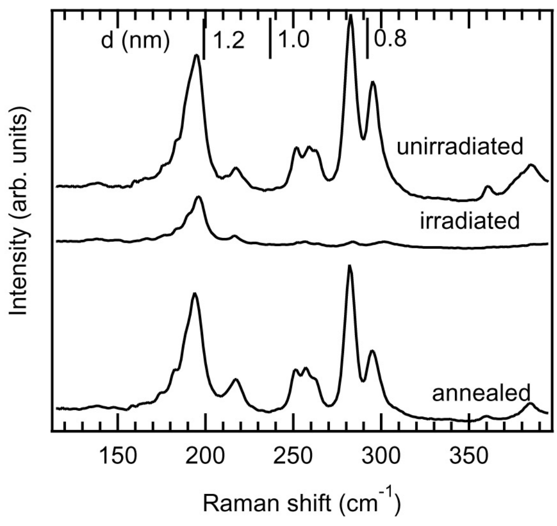

Fig. 1. Raman spectra of pristine, irradiated, and annealed SWNTs.

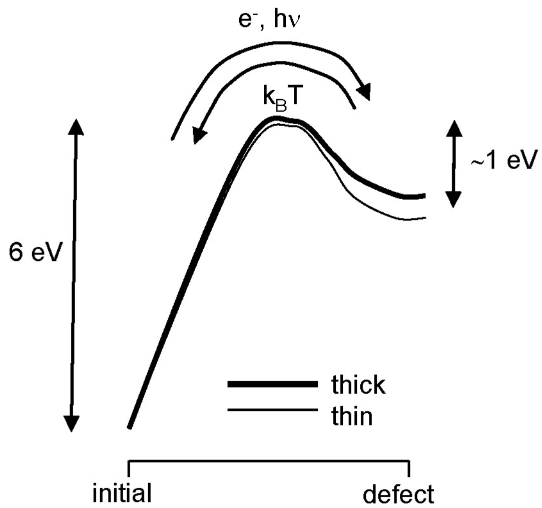

Fig. 2. Schematic energy diagram of the defect formation and healing.

Combined Scanning Tunneling and Aperture Near-field Microscopy: Tip Modeling

Ilya Sychugov and Hiroo Omi
Materials Science Laboratory

Optical and electrical properties of nanostructures can be addressed using radiation or electrical current as a probe. In general, a near-field type of electromagnetic interaction is necessary for an optical probe to enter nanoscale regime in the spatial resolution domain by overcoming the optical diffraction limit (~ 1 μm). A typical scanning near-field optical microscope (aperture-SNOM) provides such an opportunity both for the excitation and collection of light for spectroscopy applications. However, this instrument utilizes a dielectric fiber tip as an aperture, which makes it unsuitable for electrical measurements. On the other hand, a scanning tunneling microscope (STM), capable of atomic-resolution measurements by electrical current, can also cause luminescence of materials. Here, in order to realize both electrical and optical probing at nanoscale, we combine these two kinds of instruments into a single unit (Fig. 1).

In order to evaluate tip geometry influence on its performance for various operation regimes finite element method (FEM) simulations were carried out. It was found that tip transmittance for SNOM excitation mode depends strongly on tip geometry away from the edge. A variation of nearly two orders of magnitude is a result of constructive/destructive interference of the excitation light (Fig. 2). Furthermore, the role of the opening in protective metal film in light collection efficiency was simulated for the STM-luminescence mode. Based on the present simulations one can choose a suitable tip configuration from the interplay between the instrument collection efficiency and its spatial resolution [1].

We aim at concurrent optical and electrical characterization of nanostructures (e.g. quantum wells, dots, etc.) with high spatial resolution. In addition, this approach may find its niche where electrical modification with subsequent *in situ* optical probing is desirable.

[1] I. Sychugov, H. Omi, T. Murashita, and Y. Kobayashi, Appl. Surf. Sci., in press.

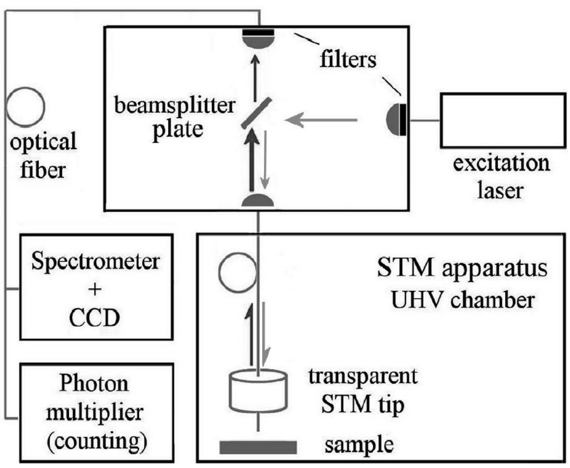

Fig. 1. Schematic representation of the setup.

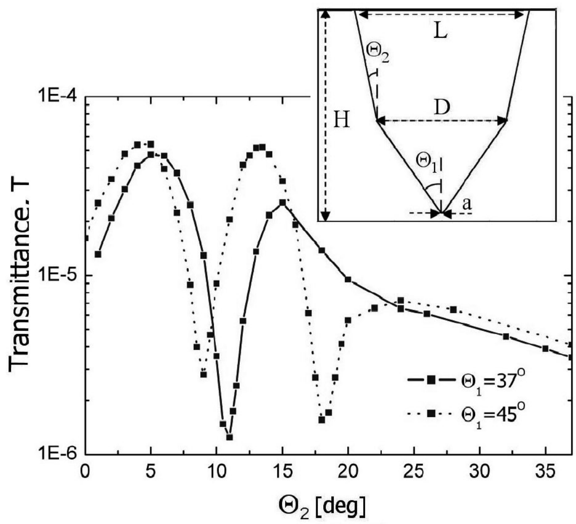

Fig. 2. Calculated tip transmittance.

Evaluation of Number of Graphene Layers Grown on SiC

Hiroki Hibino[1] and Hiroyuki Kageshima[2]
[1]Materials Science Laboratory, [2]Physical Science Laboratory

Recently, graphene has attracted much attention as a material for future electronics [1]. So far, electronic device properties have been investigated for graphene layers produced in two ways: graphene flakes exfoliated from bulk graphite [1] and epitaxial graphene grown on SiC substrates by annealing [2]. Epitaxial graphene grows on a wafer scale and is promising for device integration. To make epitaxial graphene applicable, however, we need to grow wide epitaxial graphene with the intended number of layers. As a base of this growth control, we have established a way of determining the number of graphene layers microscopically [3].

We evaluated the number-of-layers distribution in epitaxial graphene grown on SiC by low-energy electron microscopy (LEEM) using quantized oscillations of electron reflectivity. Figure 1 shows LEEM images of epitaxial graphene on 4H-SiC(0001) at various electron beam energies, which corresponds to the mappings of the secular electron reflectivity in the normal incidence. These images show that the electron reflectivities in different regions change with the energy in different manners. Figure 2 shows the energy dependence of the electron reflectivities in areas A-H. The reflectivity oscillates with the electron beam energy.

Bulk graphite has continuous electronic bands normal to the graphene sheet, but these bands split into discrete energy levels in graphene layers due to their finite thickness. When the energy of incident electrons coincides with one of the discrete energy levels, the electrons resonantly transmit through the layers, resulting in dips in the reflectivity. Therefore, the number of graphene layers can be counted directly as the number of dips in the reflectivity. The validity of this scenario was confirmed by the result that the quantized conduction band states calculated using tight-binding and first-principles methods well reproduce the dip positions in the reflectivity. *In-situ* microscopic determination of the number of graphene layers using LEEM would greatly contribute to the growth control of epitaxial graphene.

This work was partly supported by KAKENHI (19310085) from the Ministry of Education, Culture, Sports, Science and Technology of Japan.

[1] K. S. Novoselov and A. K. Geim, Nature Materials **6** (2007) 184.
[2] C. Berger, et al., Science **312** (2006) 1191.
[3] H. Hibino, et al., Phys. Rev. B **77** (2008) 075413; H. Hibino, et al., e-J Surf. Sci. Nanotechnol. **6** (2008) 107.

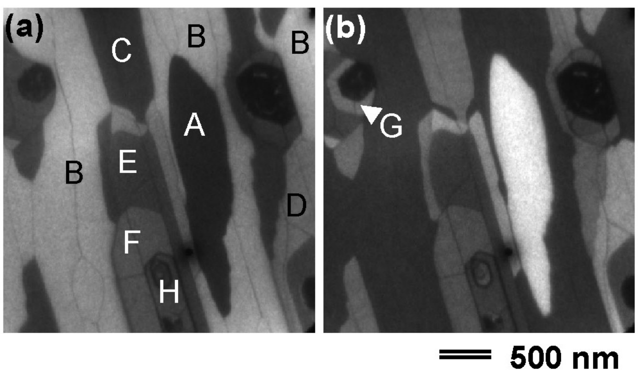

Fig. 1. LEEM images of graphene layers grown on 4H-SiC(0001) at the electron beam energies of (a) 3.0 and (b) 4.5 eV.

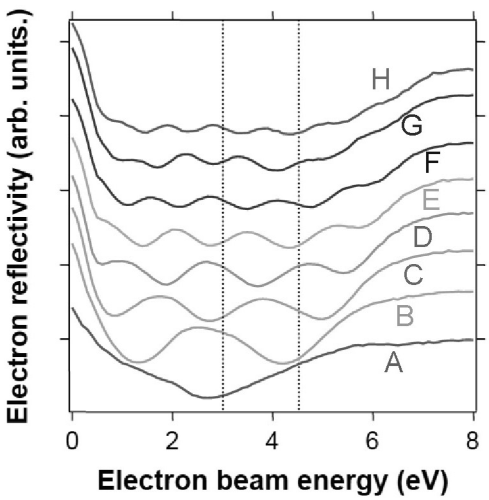

Fig. 2. Electron reflectivities in areas A-H in Fig. 1 versus the electron beam energy.

Elastic Modulus of Suspended Membrane Protein Measured by Atomic Force Microscopy

Koji Sumitomo[1], Ari M. Siitonen[1], Chandra S. Ramanujan[2], and Youichi Shinozaki[1]
[1]Materials Science Laboratory, [2]University of Oxford

Using the atomic force microscopy (AFM), we have studied the mechanics of purple membrane (PM) suspended over nanostructures. By doing this we could evaluate the properties of the biological membrane free from interaction with the substrate. Biological membranes containing lipids and proteins are important components of bio-nanostructures with many potential applications, e.g. single-molecule biosensors, and reliable measurements of their mechanical properties are essential.

PMs of *Halobacterium salinarium* strain S9 were adsorbed on a Si substrate with nano-trenches fabricated using a photolithographic technique. After locating the suspended PM using the AFM in imaging mode, force-displacement measurements were performed. Figure shows AFM images of PM suspended over nano-trenches (a) before and (b) after indentation and (c) the force-displacement curve measured during indentation. The indentation mark left by the AFM tip can be clearly seen in (b) as indicated by the arrow. As the force is increased the suspended membrane was stretched and finally punctured. The force-displacement curve during membrane stretching reflects its mechanical property directly. To evaluate the surface tension, a simple theoretical model was made, and theoretical force curves were obtained to simulate the experimental force curves. From the best-fit curve, the elastic modulus of PM was estimated to be 8 ± 1 MPa [1].

We have demonstrated that AFM measurements provide a very good approach to evaluate the mechanics of biological membranes in their native conditions. Proteins in the suspended potion of the membrane are not affected by the substrate and are more likely to function as they would *in vivo*. The next stage of this project is to measure changes in properties in response to an external stimulus such as mechanical stimulus, light irradiation, and chemical binding.

This research was supported in part by the Strategic International Cooperative Program, Japan Science and Technology Agency (JST).

[1] Ari M. Siitonen, et al., Appl. Surf. Sci., in press.

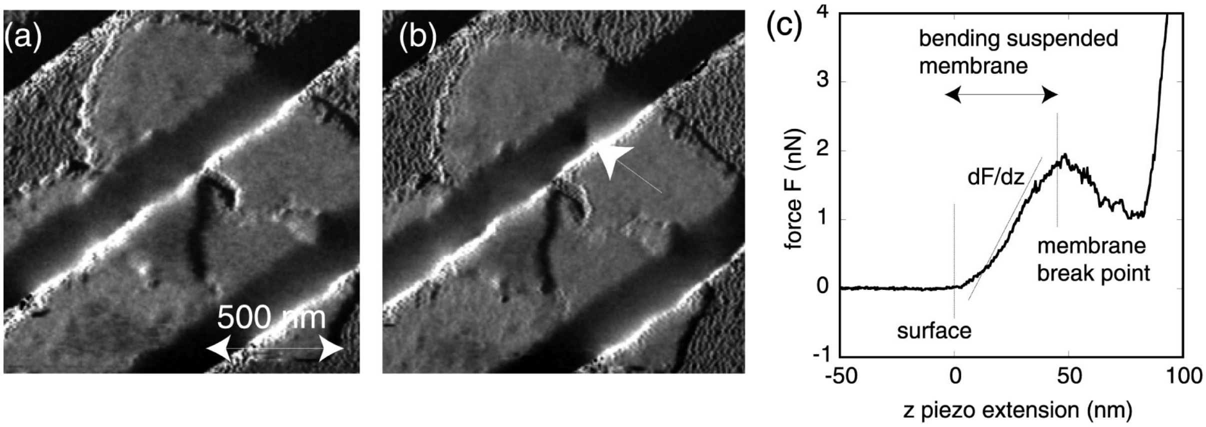

Fig. AFM images of the PM suspended over nano-trenches: (a) before and (b) after indentation; (c) the force-displacement curve measured for suspended PM.

Quantitative Analyses of FRET Efficiency of Dye Molecules Confined within 2-Dimensional Space

Kazuaki Furukawa
Materials Science Laboratory

Lipid bilayer, the fundamental component of cell membranes, can form at the solid-liquid interface by self-organization. We have developed a new type of microchannel device using this self-spreading characteristic of the lipid bilayer [1]. The validity of the device has been confirmed by observing fluorescence resonance energy transfer (FRET). This report is of the successful application of the device to the quantitative determination of FRET efficiency [2].

L-α-PC (extracted from egg yolk) containing 1 mol % of NBD- (a dye for donor) or Texas Red (TR, a dye for acceptor)-conjugated lipid is prepared. They are self-spread from the each side of the straight line pattern with a 10 μm width. Figure 1A shows the confocal laser scanning microscope images from the moment the lipid bilayers collide (set as $t = 0$) to 600 s. The observation conditions are NBD: 488 nm excitation and 505-525 nm emission, TR: 543 nm excitation and > 610 nm emission. Figure 1B plots the fluorescence intensities averaged over the widths against the position x at each time. The collision position is set as $x = 0$.

After the collision, two self-spreading bilayers are unified and form a single bilayer that provides the 2-dimensional field for the NBD- and TR-conjugated lipids to diffuse. The average fluorescence intensities can be expressed by the solution of 1-dimensional diffusion equation [2]. As the initial concentration of dye-conjugated lipids are both 1 mol % and their diffusion constants should be almost equal, the sum of the concentrations of two dye lipids are constant, 1 mol %, at any x. By analyzing the data in Fig. 1B using these reasonable assumptions, the quantitative determination of FRET efficiency depending on the donor-to-acceptor ratio becomes possible as shown in Fig. 2. A large number of data follow a unique curve, which supports the reliability of our experiments.

[1] K. Furukawa, et al., Lab Chip **6** (2006) 1001.
[2] K. Furukawa, et al., Langmuir **24** (2008) 921.

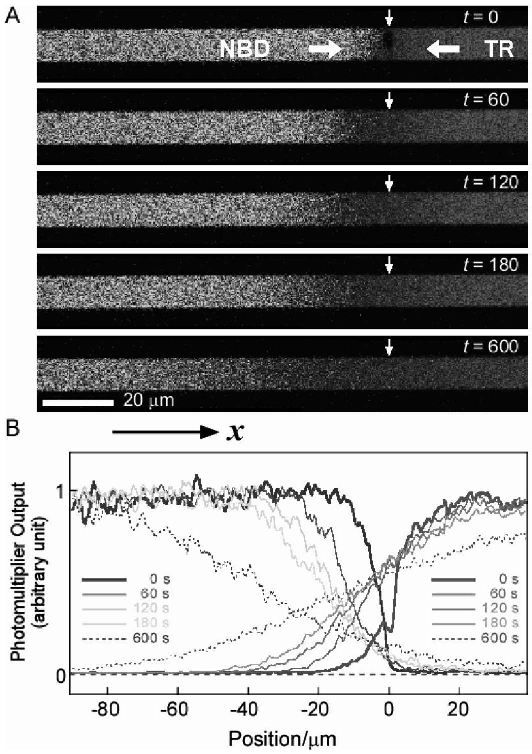

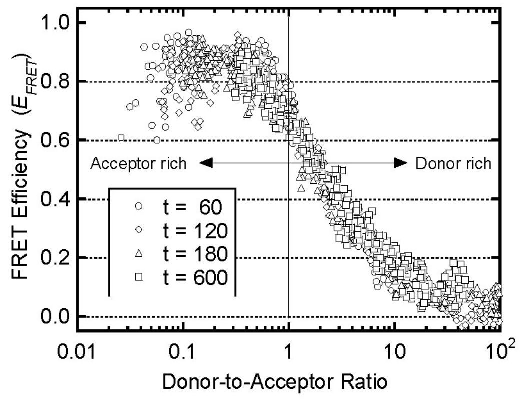

Fig. 2. (top) Donor-to-acceptor ratio dependent FRET efficiency.

Fig. 1. (left)
A. Confocal laser scanning microscope images of the self-spreading L-α-PC containing 1 mol % NBD and Texas Red before and after the collision.
B. Fluorescence intensities averaged over the 10 μm width.

AFM Observation of a Single Receptor Reconstituted into Lipid Bilayer

Nahoko Kasai[1] and Chandra S. Ramanujan[2]
[1]Materials Science Laboratory, [2]University of Oxford

Ionotropic receptors (ligand-gated ion channel receptors) are important membrane proteins for signaling in the neuronal networks of the central nervous system. They are regulated by a ligand which binds to the extracellular ligand binding domains. This binding gives an allosteric change in the structure and opens the ion channel incorporated in the transmembrane domain to allow cations flow into the cell (Fig. 1). Atomic force microscopy (AFM) enables the nano-scale observation of proteins in a liquid environment, offering a unique opportunity to observe functional biological molecule such as single proteins under physiological conditions.

In this study, we have succeeded in observing the structure of single purified and ionotropic receptor proteins in the solution using the AFM. Receptor proteins were purified from over-expressed insect cells, and then reconstituted into an artificial lipid bilayer by dialysis because the receptors would function as *in vivo* when reconstituted into the lipid bilayer. We then imaged the reconstituted receptor proteins on a substrate in a buffer solution using AFM. Before reconstitution, receptors were observed at the edge of small lipid patch on mica (Fig.2 (A)), while after the reconstitution, receptor proteins settled in the large lipid domain on mica (Fig. 2(B)) which provides for the structural observation of the single receptor. Then by zooming in on the single receptor protein, we could observe that it consisted of four protrusions suggesting the four subunits of the receptor protein.

This study demonstrates that AFM can observe functioning single ionotropic receptors, which suggests the possibility of determining a real-time conformational change of a functioning membrane protein using AFM [1].

This research was supported in part by Bio-nanotechnology IRC in U.K. and by the Strategic International Cooperative Program, Japan Science and Technology Agency (JST).

[1] N. Kasai, et al., Neurosci. Res. **58** (2007) S193.

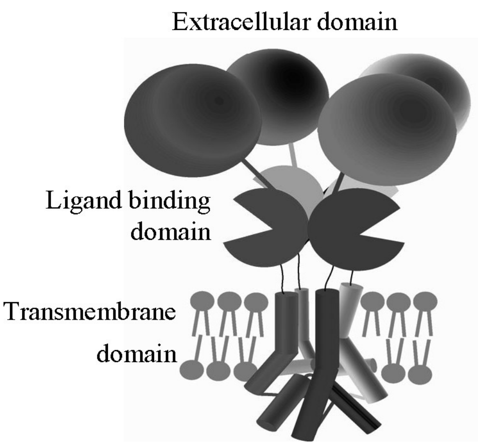

Fig. 1. Illustration of a receptor.

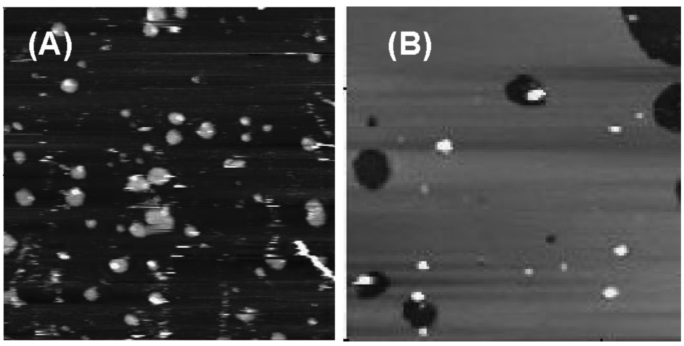

Fig. 2. AFM images of receptors before (A) and after (B) reconstituted into artificial lipid bilayer (2×2 μm). Black area: mica substrate, gray: lipid bilayer, white dots: receptor proteins.

Nanoampere Charge Pump by Single-electron Ratchet Using Silicon Nanowire MOSFET

Akira Fujiwara, Katsuhiko Nishiguchi, and Yukinori Ono
Physical Science Laboratory

Clocked transfer of single electrons is attracting a great deal of interest in its application to current standards in metrology and integrated single-electron (SE) circuits. While the conventional metal-based SE pumps and turnstiles employ fixed tunnel junctions of metal oxide, the use of gate-induced electrostatic tunable barriers in semiconductors has a clear advantage for higher-frequency operation because the tunnel resistance can be tuned to reduce the RC time. Although we showed 100-MHz operation of an SE turnstile using Si nanowire MOSFETs with two barriers modulated by two phase-shifted AC signals [1], higher-frequency operation is desired because nanoampere current is necessary for the so called metrological triangle experiment.

We recently developed a nanoampere SE pump operated based on a simple scheme using only one AC signal applied to one gate [2]. We named the proposed device an SE ratchet since it utilizes the asymmetry potential to capture electrons from the source and eject them to the drain, thereby causing directional SE transport without any source-drain bias. Figures 1(a) and 1(b) show a top-view scanning-electron-microscope (SEM) image of the device and a schematic diagram of the ratchet potential, respectively. We apply AC pulse voltage V_{G1} at frequency f to the center gate and constant lower voltage V_{G2} to the drain-side gate. SEs are captured from the source into the island, and then ejected to the drain. The number of transferred electrons per cycle is controlled by the upper gate voltage, V_{UG}. As shown in Fig. 1 (c), current plateaus ($I = mef$, m: integer) are clearly observed at 20 K in a wide range of the drain bias (V_D), which indicates that the SE transfer is directional regardless of the bias polarity. The V_D range can be much larger than the charging energy of the island (~10 meV) thanks to the potential control of the island as well as the barrier. Nanoampere charge pumping is obtained at f =2.3 GHz as shown in Fig. 2. The transfer accuracy is roughly estimated to be in the order of 10^{-2}. It is found that the nonadiabacity of the electron capture affects the shape of the current steps. This is an important finding for further study towards higher accuracy. The SE ratchet is a promising device in the application to large-current source for metrological standards. This work was partially supported by KAKENHI (16206038, 19310093).

[1] A. Fujiwara, et al., Appl. Phys. Lett. **84** (2004) 1323.
[2] A. Fujiwara, et al., Appl. Phys. Lett. **92** (2008) 042102.

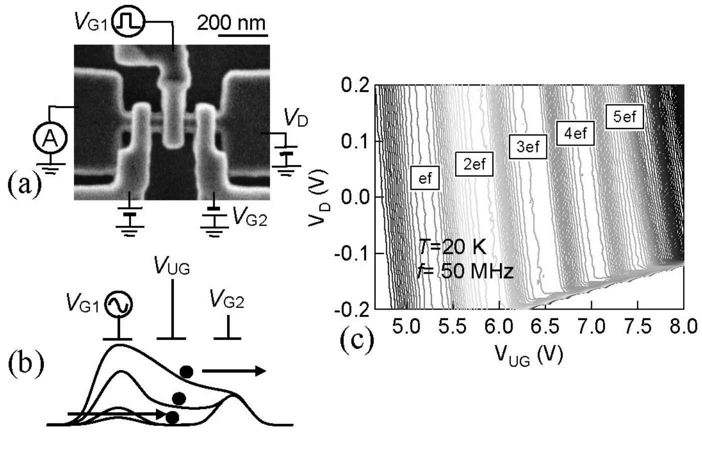

Fig. 1. (a) SEM image before upper gate formation.
(b) Schematic diagram of SE ratchet.
(c) Contour plots of current for V_D and V_{UG}.

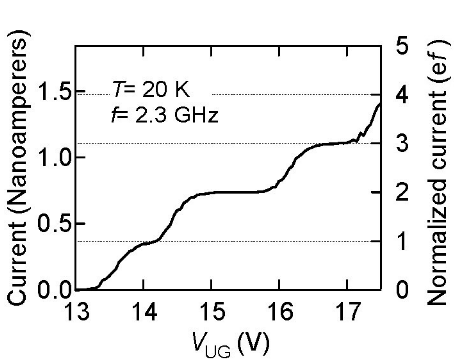

Fig. 2. Pump current at f = 2.3 GHz.

Infrared Detection with Silicon Nano-transistors

Katsuhiko Nishiguchi, Akira Fujiwara, Yukinori Ono, and Hiroshi Yamaguchi
Physical Science Laboratory

Continuously growing information technology markets have been expanding the application fields of sensor devices. Among the various kinds of sensors, Si-based image sensors using charge-coupled devices, photo diodes, and so on, have been used extensively because of their highly useful features, such as high miniaturization and integration, compared to those made of other materials. A basic mechanism of these sensors is that photons with visible wavelengths, whose energy is larger than the band gap of Si, generate electron-hole pairs. Whereas an infrared (IR) signal with wavelength longer than the visible one is useful for numerous applications, such as remote sensing, thermal sensing, and material analysis, a Si-based IR sensor is not good at detecting IR signal, compared to other sensors, because it does not have enough energy for electron-hole pairs to be generated.

We thus developed a new method of detecting an IR signal using a Si-based device [1]. The device is composed of two transistors fabricated on a silicon-on-insulator wafer (Fig. 1). The first transistor (FET1) has a two-layer gate: an upper gate (UG) is used to induce an inversion layer and a lower gate (LG) forms an energy barrier in the undoped channel of FET1. As a result, an electron-storage node (MN) electrically isolated from an electron source (ES) is formed. IR irradiation to FET1 excites electrons in the ES and some of the excited electrons diffuse into the MN over the energy barrier formed by the LG. The tiny charge originating from electrons in the MN are detected with high charge sensitivity by the other transistor (FET2), whose channel is capacitively coupled to the MN.

Figure 2 shows the change in FET2 current with and without IR radiation. The FET2 current decreased stepwise with the same height, which means that one electron, which entered the MN from the ES, was detected as one step of the FET2 current owing to the high charge sensitivity of FET2. The increase in electron injection into the MN by IR radiation means that electrons in the ES were excited and then injected into the MN over the energy barrier under the LG, which enables a function of IR-signal detection. An IR signal with shorter wavelength caused more frequent electron injection into the MN. This enables the device to function as a short-wave length pass filter by controlling the energy barrier using the LG. Additionally, since the number of electrons excited by an IR signal is proportional to electron density in the ES, which is controlled by the UG, IR signal sensitivity can be controlled by the UG. Since the demonstrated Si-based device can detect an IR signal with new functions electrically controlled by gates, its applications could be expanded to various fields.

[1] K. Nishiguchi, et al., Appl. Phys. Lett. **90** (2007) 223108.

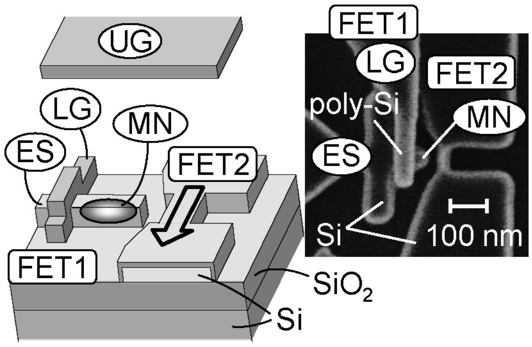

Fig. 1. IR detector device structure.

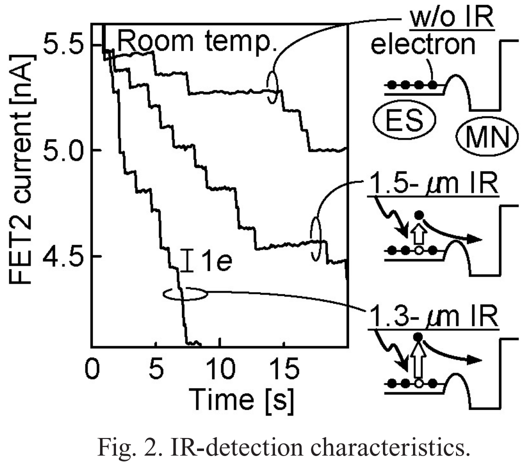

Fig. 2. IR-detection characteristics.

Detection of the Mechanical Friction Caused by Electron Systems

Hiroshi Yamaguchi[1], Hajime Okamoto[1], Sunao Ishihara[2], and Yoshiro Hirayama[1,3]
[1]Physical Science Laboratory, [2]University of Tokyo, [3]Tohoku University

Novel methods for investigating the electron behavior in low-dimensional semiconductor structures have been recently developed by integrating these structures into micro/nanomechanical systems. Using the methods, remarkable strain effects on transport properties [1] and the electron magnetization have been studied. We integrated a high mobility two-dimensional electron system (2DES) in micromechanical cantilevers to study the strain effect on magnetotransport properties in the quantum Hall regime. In addition to the remarkable strain effect at the localized-delocalized electronic state transition, we detected electron-induced internal friction against the cantilever motion with the help of the high mechanical performance of the single crystalline cantilever [2].

A 2DES Hall bar with low-temperature mobility of 2.4×10^6 cm^2/Vs was integrated near the clamping point of a 200-μm long and 60-μm wide cantilever with the thickness of 1.3 μm (Fig.1). Using a piezoelectric ceramic to drive the cantilever mechanical motion, the induced resistance change was measured as a function of magnetic field. The obtained ‘magnetopiezoresistance’ curve showed a strongly enhanced piezoresistance at the transition between the localized and delocalized electronic states. We obtained a maximum piezoresistive gauge factor of as much as 25,000 near the ν=4 transition.

We found that the cantilever mechanical motion is affected by friction exerted by the electron system, demonstrating its availability for studying the electron energy dissipation. The quality factor of mechanical resonance strongly depended on the applied magnetic field; the value was about 10^6 near the localized states but only 3×10^5 for fully delocalized states, indicating the suppression of electron energy dissipation by electron localization (Fig. 2). The strong coupling of the mechanical and electronic degrees of freedom in such integrated structures provides us with a novel method with which to undertake a detailed study of electron behavior in low-dimensional semiconductor structures.

This work was partly supported by Japan Society for the Promotion of Science (JSPS) KAKENHI (16206003).

[1] H. Yamaguchi, et al., Appl. Phys. Lett. **86** (2005) 052106.
[2] H. Yamaguchi, et al., Jpn. J. Appl. Phys. **46** (2007) L658.

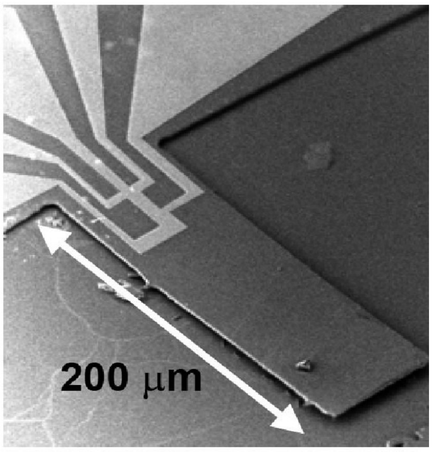

Fig. 1. Fabricated cantilever structure.

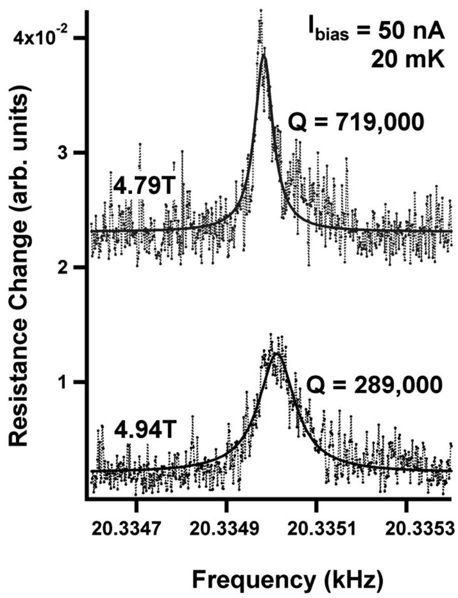

Fig. 2. Mechanical resonance.

Piezoelectric Effect on Piezoresistance of InAs/AlGaSb Heterostructure Nanobeam

Kenji Yamazaki[1], Samir Etaki[2], Herre S. J. van der Zant[2], and Hiroshi Yamaguchi[1]
[1]Physical Science Laboratory, [2]Delft University of Technology

Nanoelectromechanical systems (NEMS) are attracting much interest as sensors with very high sensitivities and as new-principle devices. Our group has reported mechanical systems using InAs/AlGaSb heterostructures and sensitivity enhancement using quantum effects on electrons in the structures. However, the basic mechanism of piezoresistance (i.e., resistance change due to mechanical strain) in such systems has not been understood well. In this study, we fabricated InAs/AlGaSb NEMS and measured/analyzed its piezoresistance. The results strongly imply that the piezoresistance in such systems is significantly affected by the piezoelectric effect and thus reveale, for the first time, the importance of the piezoelectric effect in mechanical systems using very thin heterostructures.

Figure 1 shows an atomic force microscopy (AFM) image of a fabricated double-clamped nanobeam made of an InAs/AlGaSb heterostructure. The thicknesses of InAs and AlGaSb layers are 15 and 35 nm, respectively. Depending on the depth of wet etching, which makes the nanobeam suspended, the shape of the beam becomes straight or arched. This is because the shear stress due to the lattice mismatch curls the wide suspended supports upward, and the beam linking the two supports thus becomes arched. The piezoresistance measured using an AFM tip for deflecting the beam had large dependence on the beam shape. That is, the gauge factor (GF) derived from the resistance change and strain, which usually reflects material properties, was positive or negative depending on whether the beam was straight or arched, and the magnitude was much larger than for bulk (See Table) [1]. To try to understand these surprising phenomena, we calculated the piezoresistance, including the piezoelectric effect (Fig. 2). The results suggest that the piezoresistance is significantly affected by the piezoelectric effect for heterostructure thin film. That is, additional charges on the beam surface, which are induced by the piezoelectric effect when the structure is strained, change the resistance, and this effect is larger when the conductive layer is thinner and thus the carrier density is lower. Moreover, the opposite signs were also obtained for the arched and straight beams by calculation, which means that our understanding roughly explains the experimental results.

These results enhance our understanding of piezoresistance in NEMS, which could lead to more effective designs for them.

This work was supported in part by Japan Society for the Promotion of Science (JSPS) KAKENHI(16206003) and the Dutch NWO VICI-grant.

[1] K. Yamazaki, S. Etaki, H. S. J. van der Zant, and H. Yamaguchi, J. Cryst. Growth **301-302** (2007) 897.

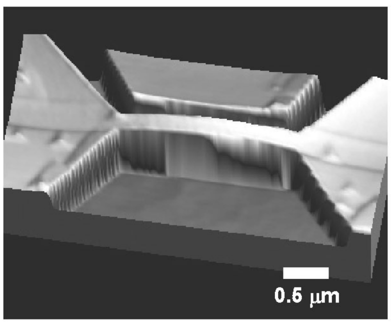

Fig. 1. AFM image of fabricated 50-nm-thick arched beam.

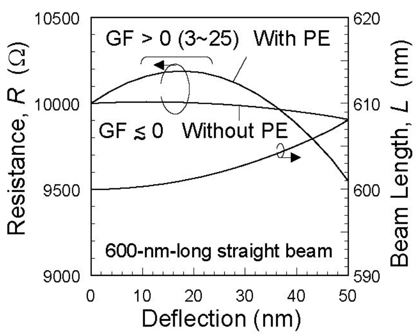

Fig. 2. Calculated resistance with and without the piezoelectric effect (PE).

Table. Measured gauge factor ($GF = (\Delta R/R)/(\Delta L/L)$).

		GF
This study	Arched beam	
	600-nm long	–4.8
	2-μm long	–3.3
	Straight beam	
	500-600-nm long	+7.2
	1-μm long	+3.7
Bulk InAs		–0.9

Electron Spins in Bilayer Quantum Hall Systems Investigated by Nuclear Spin Measurements

Norio Kumada[1], Koji Muraki[1], and Yoshiro Hirayama[2]
[1]Physical Science Laboratory, [2]Tohoku University

Two-dimensional electron system (2DES) formed in a high-mobility semiconductor heterostructures can be an ideal laboratory to study many-body phenomena in low dimensions. In a quantum Hall (QH) system, which appears by applying magnetic field perpendicular to a 2DES, the kinetic energy of electrons is quantized into Landau levels and electron-electron interactions completely dominate physics. In particular, in a bilayer system consisting of closely separated 2DESs, interplay between the spin and layer degrees of freedom leads to various broken symmetry states called QH magnets. We developed nuclear magnetic resonance (NMR) techniques for QH systems and studied static and dynamic properties of electron spin in QH magnets [1-3].

NMR is commonly used as a powerful probe of spin states in various electronic systems. For QH systems, however, a small number of nuclei in contact with the 2DES have restricted NMR measurements to multiple-layer samples. To perform NMR in a bilayer QH system, we exploit current-induced nuclear spin polarization and its resistive detection. The Knight shift of the NMR spectrum, which is proportional to the electron spin polarization, shows the existence of the canted antiferromagnetic state between the ferromagnetic and spin-singlet states with full and null spin polarizations, respectively (Fig. (a)). Furthermore, the nuclear spin relaxation rate reveals that, in the canted antiferromagnetic state, low-frequency electron spin fluctuations do not freeze out even in the low-temperature limit (Fig. (b)). The collective fluctuation at low temperature is characteristic behavior of broken symmetry states in two dimensions.

[1] N. Kumada, et al., Phys. Rev. Lett. **94** (2005) 096802.
[2] N. Kumada, K. Muraki, and Y. Hirayama, Science **313** (2006) 329.
[3] N. Kumada, K. Muraki, and Y. Hirayama, Phys. Rev. Lett. **99** (2007) 076805.

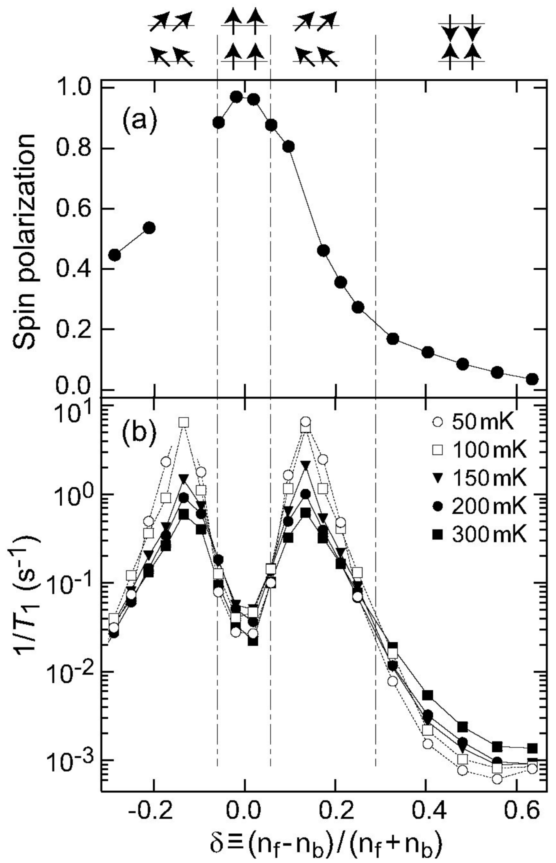

Fig. (a) Electron spin polarization and (b) nuclear spin relaxation rate measured by NMR. The nuclear spin relaxation rate reflects electron spin fluctuations.

Imaging Percolation of Localized States in a Semiconductor Quantum Well

Simon Perraud[1,2], Kiyoshi Kanisawa[1], Zhao-Zhong Wang[2], and Toshimasa Fujisawa[1]
[1]Physical Science Laboratory, [2]LPN-CNRS

One of the advantages of two-dimensional electron system (2DES) formed in semiconductor heterostructures is the possibility to control the main system parameters, including electron confinement tuned by varying the thickness of the grown layers and electron density tuned by applying an external electric field. Recently, we found that the Fermi level was mostly unpinned at the (111)A clean surface of n-type $In_{0.53}Ga_{0.47}As$ [1]. Therefore, it could be possible to vary the electron density in the (111)A-oriented $In_{0.53}Ga_{0.47}As$ surface quantum well (QW) to access 2DES by using scanning tunneling spectroscopy (STS) measurements in the ultra-high vacuum (UHV). This allows us to perform studies of electron phenomena in disordered 2DES at the nanometer-scale spatial resolution. The effect of disorder is very important to understand various electron behaviors, especially the many-body phenomena in the semiconductor structures.

An $In_{0.53}Ga_{0.47}As/In_{0.52}Al_{0.48}As$ multi-subband surface QW was grown by molecular beam epitaxy on lattice-matched InP(111)A substrate, and the electronic local density of states (LDOS) in this QW was measured at 5 K by low-temperature STS in UHV. The LDOS in the conduction band has a clear step-like energy dependence, revealing that 2DES subbands are formed in the QW (Fig. 1). At a given energy, the LDOS shows strong spatial fluctuations in the QW plane due to the presence of a disorder potential. The formation of the localized states is due to quantum-mechanical interference between electron waves that have undergone multiple scatterings by the disorder potential. Percolation of localized states with increasing energy is observed in each subband tail. This percolation is explained by using a semiclassical model. The origin of the disorder potential is ascribed to a random distribution of native point defects located at the QW surface [2].

This work was partly supported by a Grant-in-Aid for Scientific Research from the Japan Society for the Promotion of Science, JSPS KAKENHI (16206003).

[1] S. Perraud, et al., Appl. Phys. Lett. **89** (2006) 192110.
[2] S. Perraud, et al., Phys. Rev. B **76** (2007) 195333.

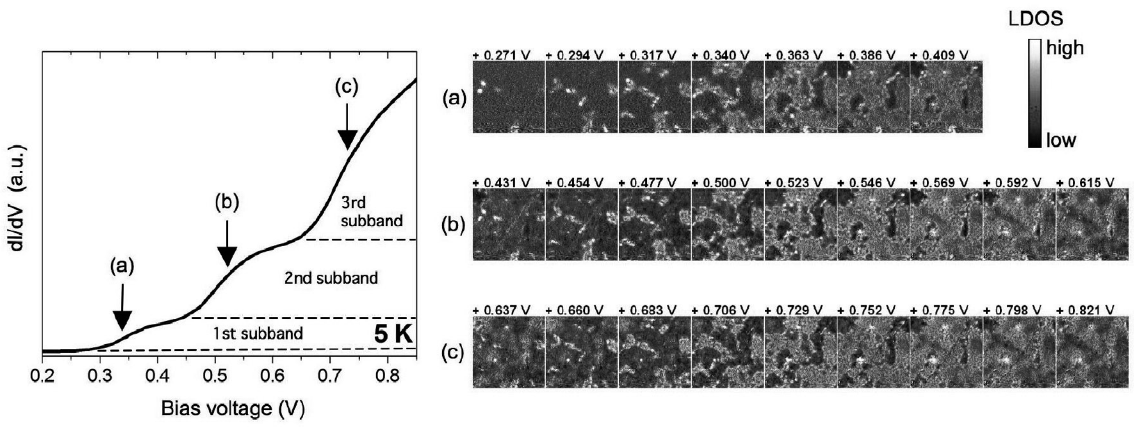

Fig. 1. Measured *dI/dU* spectrum averaged over the whole area (214 nm × 214 nm) of the InGaAs surface QW at 5 K in UHV. Each arrow indicates the percolation threshold of each subband calculated by the semiclassical model. Observed *dI/dU* spatial maps at several values of *U* covering the transition (a) from the band gap to the first subband, (b) from the first to the second subband, and (c) from the second to the third subband.

Persistent Supercurrent Atom Chip

Tetsuya Mukai[1], Christoph Hufnagel[1], and Fujio Shimizu[2]
[1]Physical Science Laboratory,
[2]The University of Electro-Communications/NTT Research Professor

Neutral single atoms are promising candidate for producing quantum devices. An important technology for developing these quantum devices is a precise control of the external motion of each single atom. In general, room temperature (300 K) atoms are moving with relatively high speed at around 1,000 km/h, but with laser cooling techniques, atoms can be quickly decelerated to velocities slower than the walking speed of a human being, i.e., lower than 100 μK in temperature. At such a low temperature gravitational acceleration is significant and atoms start falling down just like a macroscopic object.

Atoms with non-zero magnetic moment have weak field-seeking states. They can be trapped with a magnetic potential which competes against the gravity. The magnetic potential can be easily generated by a current. It is widely used for trapping large number of atoms. However, trapping single atoms with a magnetic field generated by a current has never been successful because of the short lifetime caused by the current noise. This is significant in a short atom-surface distance which is suitable for making strong confining single atom traps.

Recently, we have succeeded in developing a persistent supercurrent atom chip and trapping of atoms in the vicinity of a solid surface with a practically noise free magnetic field which is highly expected to trap single atoms. As plotted in Fig. 1, 0.5 million rubidium atoms are trapped about 300 μm away from the atom chip surface, on which a trap is generated by driving a persistent current of 2.5 Ampere through a MgB_2 superconducting loop circuit on a sapphire substrate. Apart from trapping atoms with a persistent supercurrent, we have also succeeded in controlling the persistent current with an on-chip thermal switch driven by a laser (Fig. 2) [1].

In future we will miniaturize the atom chip pattern and try to make single atom traps with a persistent supercurrent on a solid surface as a resource for quantum devices.

This research is partially supported by the Japan Science and Technology Agency CREST "Creation of new technology aiming for the realization of quantum information processing systems".

[1] T. Mukai, C. Hufnagel, et al., Phys. Rev. Lett. **98** (2007) 260407.

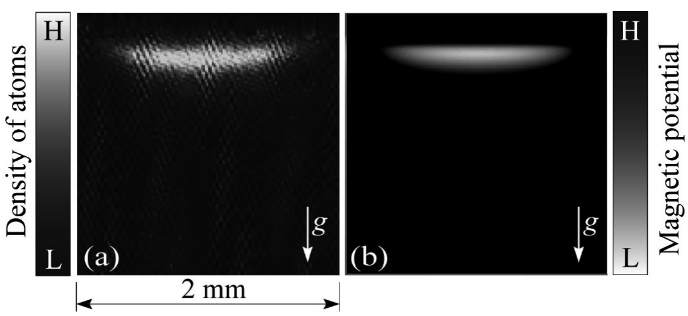

Fig. 1. Trapped atoms: (a) experiment and (b) calculation.

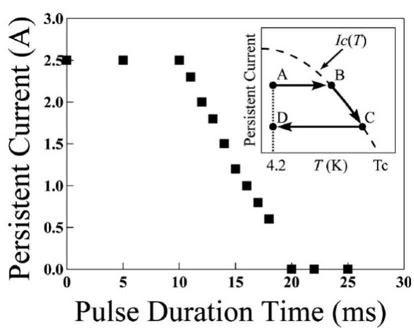

Fig. 2. Persistent current control.

A Selective and Long-distance Coupling Scheme for Plural Flux Quantum Bits

Hayato Nakano[1], Kosuke Kakuyanagi[1], Kouichi Semba[1], and Masahito Ueda[2]
[1]Physical Science Laboratory, [2]Tokyo Inst. Tech./NTT Research Professor

A quantum computer is composed of many two-state elements called quantum bits (qubits). A quantum calculation should be completed within the coherence time (during which, the quantum superposition is maintained). To achieve this, two-qubit operations where we can choose two arbitrary qubits from a large number are advantageous. Moreover, there is a strong need for an operation that can be performed even if the two qubits are not next to each other. However, to achieve two-qubit operation, we employ the physical interaction between the two qubits, therefore performing a qubit operation on a spatially remote pair is usually very difficult.

We developed a structure and an operating principle to enable such two-bit operation for superconducting qubit systems, and clarified the physical characteristics by theoretical analysis (Fig. 1) [1].

Every qubit interacts with the same superconducting resonance circuit (e.g. an LC circuit or a transmission line), but the resonance frequencies of individual qubits are sufficiently different to ignore direct interactions between qubits. We use indirect interaction through this resonance circuit and realize the function described above.

Assume that a two-bit operation is performed only between a specific qubit pair (with frequencies of ω_1, and ω_2). It is important that the resonance frequency ω_r can be varied by changing the dc bias-current (I_b) supplied to the Josephson junction in the resonance circuit. When the resonator frequency is tuned to $\omega_r \sim (\omega_1 + \omega_2)/2$ and a microwave with the frequency $\omega_{ex} \sim (\omega_2 - \omega_1)/2$ is applied from the outside, the two qubits are operated without affecting a state of a resonance circuit via a two-photon Rabi process. This means that it is possible to operate two qubits that do not interact directly.

Because only a qubit pair that simultaneously satisfies the two above ω_r and ω_{ex} conditions can react, we can choose two of specified qubits by tuning the resonator and the microwave (Fig. 2). In addition, this enables the two-bit operation of spatially longer-distance remote qubits because the resonance circuit can be 1 mm for an LC circuit [2], or more for a transmission line. This work was partially supported by CREST-JST, JSPS-KAKENHI (18201018, 18001002).

[1] H. Nakano, K. Kakuyanagi, M. Ueda, and K. Semba, Appl. Phys. Lett. **91** (2007) 032501.
[2] J. Johansson, S. Saito, T. Meno, H. Nakano, M. Ueda, K. Semba, and H. Takayanagi, Phys. Rev. Lett. **96** (2006) 127006.

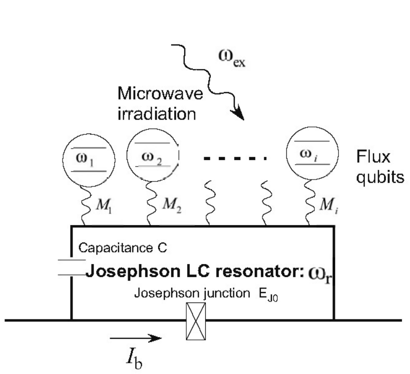

Fig. 1. Schematic structure of our coupler.

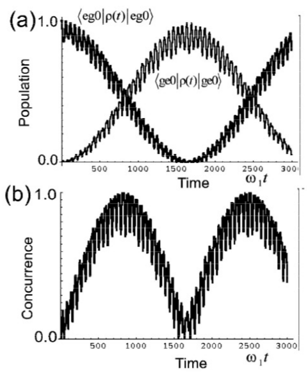

Fig. 2. Example of a two- operation (entanglement formation).

Energy Distribution Measurement of Nonequilibrium Carriers Using a Quantum Dot

Toshiyuki Kobayashi[1,4], Shoei Tsuruta[1,3,4], Satoshi Sasaki[1], Toshimasa Fujisawa[1], Yasuhiro Tokura[2], and Tatsushi Akazaki[1,4]
[1]Physical Science Laboratory, [2]Optical Science Laboratory, [3]Tokyo University of Science, [4]JST-CREST

A semiconductor quantum dot (QD) confines electrons in a nanometer-scale region. This results in discrete quantized energy levels of electrons in a QD. These quantized energy levels can be easily tuned by controlling the gate voltage, thus enabling us to use a QD as a high-resolution energy analyzer (or spectrometer) for the electrons near the QD.

We used this feature of QDs to measure the energy distribution of ballistic nonequilibrium electrons and holes emitted from a quantum wire (Fig. 1). Nonequilibrium carriers were emitted by applying a bias voltage (V_{pc}) to a quantum point contact. The emitted current was again focused by applying a perpendicular magnetic field ($B_{\perp}$) and analyzed with a QD (Fig. 2). When the energy of the nonequilibrium carriers coincides with the quantized energy levels, those carriers can resonantly tunnel through the QD and can be detected as an electric current. Therefore, when the quasi-chemical potential of the carriers is aligned at the energy levels of the QD, the differential conductance of the QD exhibits a peak and appears as a Coulomb diamonds (Fig. 3).

We found that when the bias energy is small, the energy distribution does not broaden. However, at a high bias (~1 meV), the distribution broadened owing to enhanced electron-electron scattering, which causes carrier energy relaxation [1]. This result is important for future experiments related to quantum information transfer between quantum bits.

[1] T. Kobayashi, et al., Phys. Stat. Sol. (c) **5** (2008) 162.

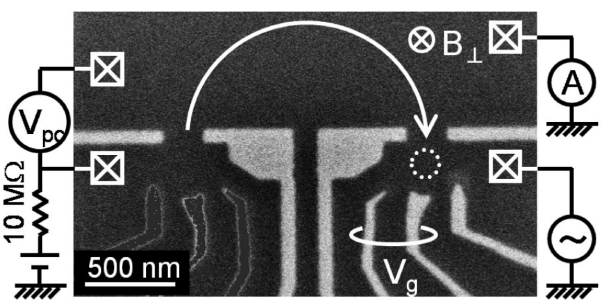

Fig. 1. Scanning electron micrograph of device and measurement setup.

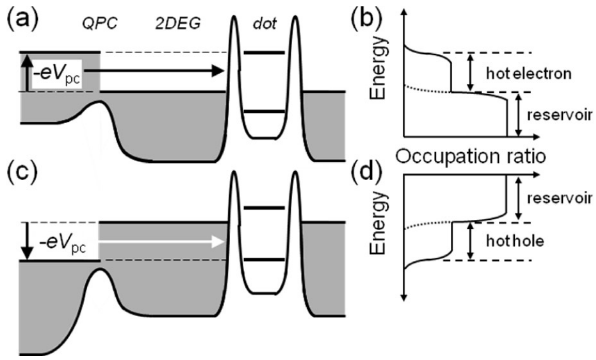

Fig. 2. (a,b) Electron accumulation and (c,d) hole accumulation near quantum dot.

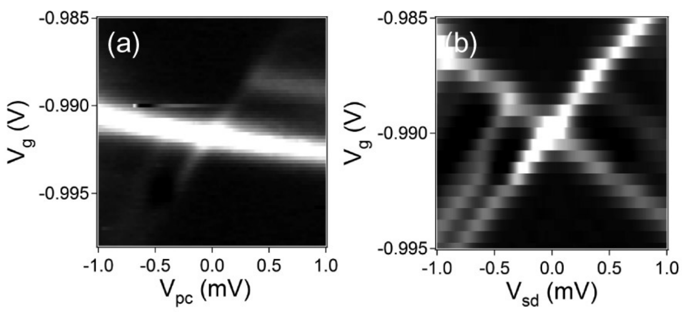

Fig. 3. (a) Coulomb diamond realized by ballistic hot carrier injection. Arrows indicate peaks caused by hot carriers tunneling through QD levels. (b) Normal Coulomb diamond by V_{sd}.

Density Dependence of Electron and Hole Effective Masses in GaAs Gated Quantum Well

Masumi Yamaguchi[1,2] and Shintaro Nomura[2,3]
[1]Physical Science Laboratory, [2]CREST-JST, [3]University of Tsukuba/NTT Research Professor

Several scattering mechanisms, such as scattering by surface charge and by donor ions, interfacial scattering, and the impurity scattering, limit the electron mobility of semiconductors. In the case of the conventional semiconductor hetero-junction, the scattering by donor ions at the doped layer causes an unavoidable reduction of the electron mobility at low electron density. The enhancement of the electron effective mass or the increase in the spin susceptibility, which has been observed by the Subnikov-de Hass oscillation measurements at low electron density, is attracting much attention in the semiconductor physicists. However, it is hard to observe them with low-mobility samples since these phenomena are induced by electron–electron interaction. Because our gated undoped quantum well has no donor layer, a high mobility is maintained even at low electron density and the electron density can be controlled continuously by the gate bias. In addition to conventional electric transport measurements, we performed photoluminescence measurements over the insulator to metallic regime by changing the electron density (n_s). We determined the electron and hole effective masses within a wide range of the electron density [1].

The electron and hole effective masses in the low magnetic field regime were obtained from the Landau level splitting of the photoluminescence peaks (Fig. 1). An increase of the electron effective mass with decreasing electron density was obtained at $n_s < 1\times10^{11}$ cm^{-2} (Fig. 2). Moreover, we found that the hole effective mass also increases with decreasing electronic density and that the hole is localized at $n_s < 3\times10^{10}$ cm^{-2}.

Using this gated quantum well, we are exploring the spin polarized state predicted to appear due to the electron-electron interaction in ultralow electron density.

[1] S. Nomura, et al., Phys. Rev. B **76** (2007) 201306R .

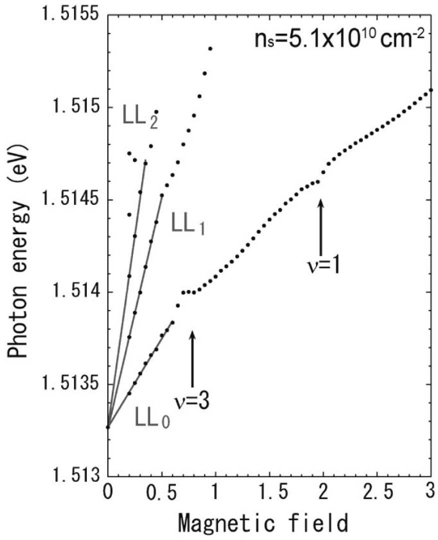

Fig. 1. Landau level fan obtained from the photoluminescence peaks.

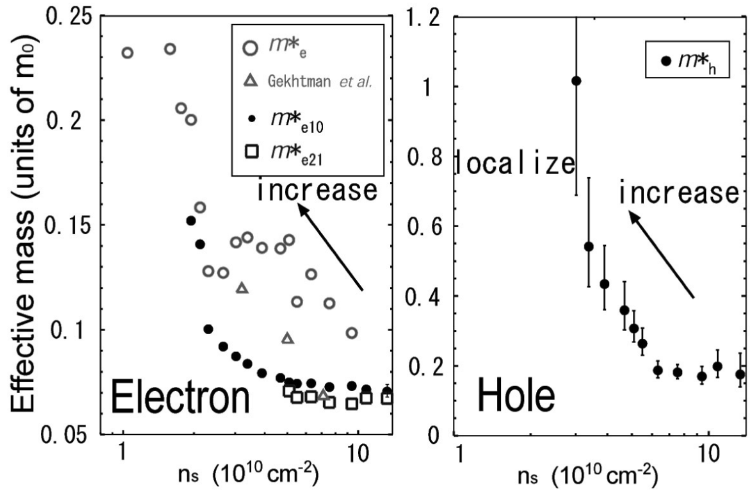

Fig. 2. Electron and hole effective masses

Quantum Key Distribution over 200 km of Fiber

Hiroki Takesue[1], Sae Woo Nam[2], Qiang Zhang[3], Robert H. Hadfield[2],
Toshimori Honjo[1], Kiyoshi Tamaki[1], and Yoshihisa Yamamoto[3]
[1]Optical Science Laboratory, [2]NIST, [3]Stanford University

It is important to establish the technologies to increase key distribution distance and key rate for realizing practical quantum key distribution (QKD) systems. We have recently demonstrated a 200-km QKD, which set the world record of key distribution distance, using a 10-GHz clock system and superconducting single photon detectors (SSPD) [1].

Figure 1 shows the system configuration, in which the differential phase shift (DPS) protocol is implemented [2]. At Alice's site, a continuous light is modulated into 10-GHz clock pulses using a high-speed intensity modulator, and the phase of each pulse is randomly modulated by $\{0, \pi\}$. Then, the pulses are attenuated so that the average photon number per pulse becomes 0.2, and sent to Bob through an optical fiber. Bob inputs the pulse train into a 1-bit delayed interferometer with which he can measure the phase differences of adjacent pulses: if the phase difference is 0 (π), the photon output from port 1 (2) and is detected by SSPD1 (2). Then, Bob informs Alice the time instances in which he observed photons through a conventional communication line. As a result, Alice and Bob share the phase difference information at those time slots, which can be converted to "keys" for one-time pad cryptography.

The working principle of the SSPD is explained as follows. When a photon hits a current-biased superconducting NbN nanowire, it "breaks" the superconductivity, and a macroscopic voltage pulse is generated. By discriminating the voltage pulse, we can detect the arrival of the photon. Although the current quantum efficiency is relatively small (about 1 %), the SSPD has very low dark count rate (about 10 Hz), and so is suitable for long-distance QKD. In addition, the SSPD can detect the 10-GHz clock signal without suffering from errors due to inter-bit interference, thanks to its good timing resolution (60 ps).

Figure 2 shows the obtained secure key rate as a function of the fiber length. Here, the secure key rate was calculated based on a security model considering general individual attacks [3]. We successfully distributed secure keys over 200 km of fiber. In addition, we obtained 17-kbit/s secure key rate at 105 km of fiber, which is two orders of magnitude larger than the previous bit-rate record at 100 km of fiber.

This research was supported in part by CREST program of Japan Science and Technology Agency and National Institute of Information and Communications Technology of Japan.

[1] H. Takesue, et al., Nature Photonics **1** (2007) 343.
[2] K. Inoue, E. Waks, and Y. Yamamoto, Phys. Rev. Lett. **89** (2002) 037902.
[3] E. Waks, H. Takesue, and Y. Yamamoto, Phys. Rev. A. **73** (2006) 012344.

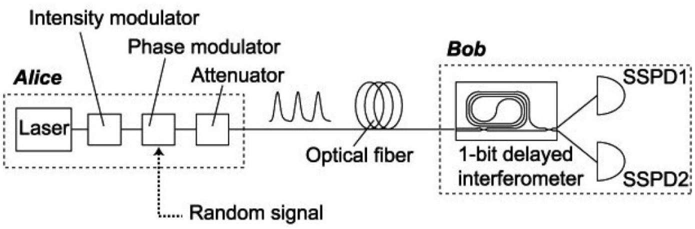

Fig. 1. System configuration.

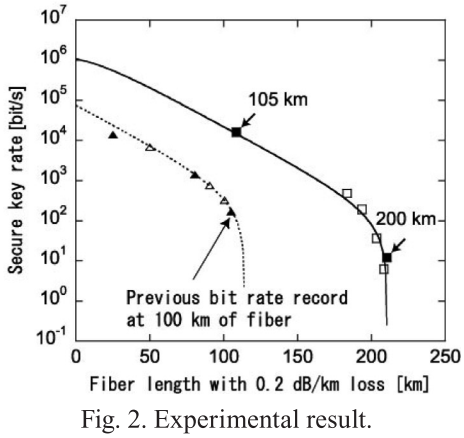

Fig. 2. Experimental result.

Field Trial of Differential-phase-shift Quantum Key Distribution Using Polarization Independent Frequency Up-conversion Detectors

Toshimori Honjo[1], Shuto Yamamoto[2], Takashi Yamamoto[2],
Hidehiko Kamada[1], Yoshiki Nishida[3], Osamu Tadanaga[3], Masaki Asobe[3], and Kyo Inoue[4]
[1]Optical Science Laboratory, [2]NTT Network Innovation Laboratories,
[3]NTT Photonics Laboratories, [4]Osaka University/NTT Research Professor

Quantum key distribution (QKD) has been studied as a way to realize unconditionally secure communications. We had been intensively working on differential-phase-shift QKD (DPS-QKD) experiment where randomly phase-modulated coherent pulse stream was used [1, 2]. Recently, we performed a field trial of DPS-QKD using polarization independent frequency up-conversion detectors to show the feasibility of our QKD scheme [3].

In this experiment, a sender generated a 1-GHz coherent pulse stream, and each pulse was randomly phase-modulated by 0, π . The pulse was attenuated to 0.2 photons per pulse and then transmitted to a receiver's site over the 17.6-km installed fiber. At the receiver's site, the pulse stream was input into a planar lightwave circuit Mach-Zehnder interferometer. The output ports of the interferometer were connected to the polarization independent up-conversion detectors. Figure 1 shows the setup of our detector. A signal pulse (photon) was input into a polarization beam splitter (PBS), which split the polarization of the incoming photon into horizontally and vertically polarized pulses. The horizontally polarized pulse was directly input into a 50:50 coupler. The vertically polarized pulse was input into a fiber delay line as a horizontally polarized pulse. After 50:50 coupler, horizontally polarized pulses were combined with a strong pump light, and injected into a periodically poled lithium niobate (PPLN) waveguide. In the PPLN waveguide, a 600 nm photon was generated via the sum frequency generation (SFG) process. After suppressing the pump, the SFG photon was detected with a single photon counting module (SPCM) based on a Si-APD. The detected signals were input into a time interval analyzer to record the photon detection events.

With this setup, we performed a long-term stability test. We successfully demonstrated stable operation for 6 hours and achieved a sifted key generation rate of 120 kbps and an average quantum bit error rate of 3.14 %, which revealed the feasibility of our QKD scheme.

This research was supported in part by National Institute of Information and Communications Technology of Japan.

[1] K. Inoue, et al., Phys. Rev. A **68** (2003) 022317.
[2] H. Takesue, et al., New J. Phys. **7** (2005) 232.
[3] T. Honjo, et al., Opt. Express **15** (2007) 15920.

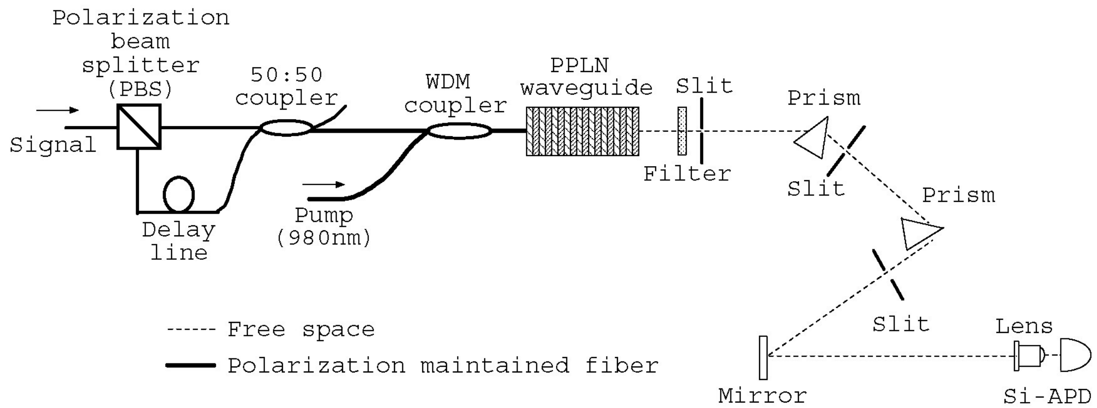

Fig. 1. Polarization independent frequency up-conversion detector.

Topology of Exciton in Artificial Structure

Masami Kumagai
Optical Science Laboratory

Topology of an electron wavefunction in artificial structures is determined by the structural parameters if the disturbance of the electron can be neglected [1]. The topology of an exciton wavefunction, however, heavily depends on the delocalized feature of the relative motion of an electron-hole pair making an exciton as well as the structural parameters. We focused our eyes to this situation and investigate the topological aspects of the exciton in nanotube structures [2].

It has been demonstrated that the exciton wavefunction shows variety of spatial distribution patterns depending on the structural parameters of the nanotube structure. We found that the origin of the change of the exciton wavefunction by controlling the tube circumference length comes from the topological transition. As shown in Fig. 1, the kinetic energy of the ground state exciton in nanotubes decreases monotonically when the circumference length decreased. This is somewhat curious because smaller confinement region yields larger confinement kinetic energy in conventional artificial structures. The exciton wavefunction is delocalized and it is connected in small circumference nanotubes, while the exciton wavefunction is localized in large circumference ones. The connected wavefunction has ring-like topology and it yields the flat wavefunction for a ground state electron and exciton reducing the confinement energy.

We have also found that the topological transition can be controlled even by changing the barrier dielectric constant of the nanotubes. Figure 2 plots the ground state exciton wavefunctions on developments of two nanotubes with different barrier dielectric constants, 12 and 3. It can be clearly seen that the wavefunction of ε=12 case is delocalized in the direction of circumference (horizontal in the figure) and connected, while the wavefunction of ε=3 case is localized in a small area and disconnected. This implies that we can control the topology of the exciton wavefunction simply by changing the dielectric constant or other material parameters. We expect the control of the artificial structure to provide a novel guiding principle for creating functional devices through the topological control of excitons.

[1] M. Kumagai and T. Ohno, Solid State Commun. **83** (1992) 837.
[2] M. Kumagai, et al., Solid State Commun. **145** (2008) 154.

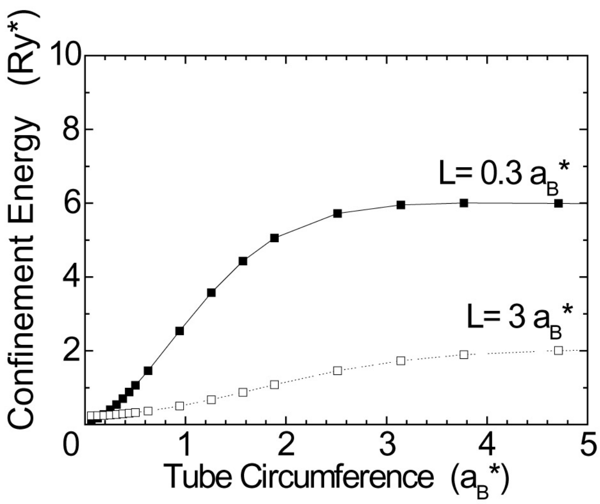

Fig. 1. Tube circumference dependence of the confinement energy.

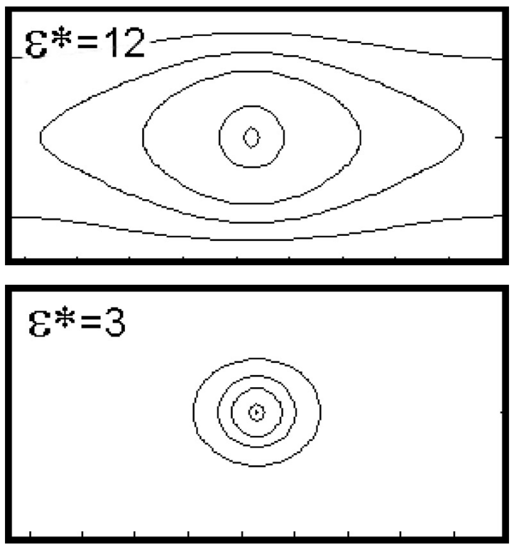

Fig. 2. Topological control of exciton by changing dielectric constant.

Efficient and Low Noise Single-photon Detection in 1550-nm Communication Band by Frequency Upconversion in Periodically Poled $LiNbO_3$ Waveguides

Hidehiko Kamada
Optical Science Laboratory

In recent years, the increasing demand for secure communication has accelerated the development of a new generation of telecommunication techniques based on quantum mechanics. Specifically, quantum key distribution (QKD) is expected to be a key technology; practical fiber-based QKD systems have been intensively studied in the 1500-nm wavelength band. For distributing keys over a long distance at a high rate, efficient and low noise single-photon detection is important. We demonstrate 1500-nm band single photon detection with low dark count noise and a potentially high efficiency. By developing frequency up-conversion devices based on sum-frequency generation (SFG) in periodically poled $LiNbO_3$ (PPLN) waveguide, which are specifically designed to use a pump wavelength longer than that of communication-band photons, we eliminate the dark count noise caused by parasitic nonlinear processes in the waveguide [1].

Periodic poling relaxes the wavenumber mismatch among three waves, thus realizing quasi-phase matching (QPM), and tight mode confinement in a LN waveguide enhances the SFG. Our devices are specifically designed to use a pump wavelength at 1810 nm. The PPLN wafers were fabricated by directly bonding a thin periodically poled wafer to a $LiTaO_3$ cladding wafer. Subsequently, the bonded wafer was cut into pieces, then a series of 7-µm thick, 6~8-µm wide and 35 or 50-mm long ridge stripes were defined with a dicing saw.

We observed internal conversion efficiency as high as 40 % (Fig. 1, 2), and demonstrated scaling down to the single photon level. Favored by long wavelength pump, which never induces parasitic χ^2 process thus eliminates the noise photons in 1500-nm band. By carefully eliminate noise photons from the pump laser, a background dark count rate less than 10^2 sec^{-1} was achieved (Fig. 2). Using the as-measured coupling of 65~70 % of a 1500-nm wave into the waveguide, and a Si-APD efficiency of ~57 %, we predict an overall photon detection efficiency of about 34~40 %.

This work was partly supported by NICT.

[1] H. Kamada, M. Asobe, T. Honjo, H. Takesue, Y. Tokura, Y. Nishida, O. Tadanaga, and H. Miyazawa, Opt. Lett. **33** (2008) 639.

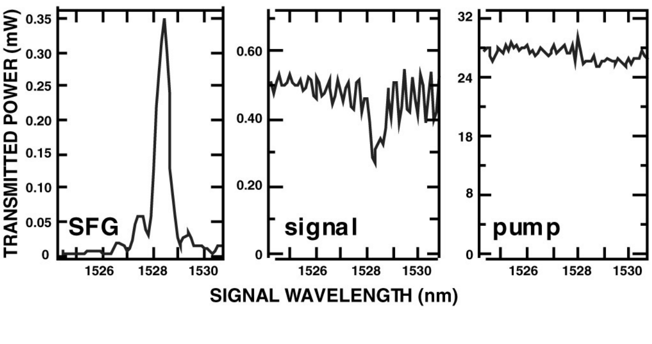

Fig.1. SFG output power (left), transmitted signal (middle) and pump (right). The temperature was set at 24 ˚C.

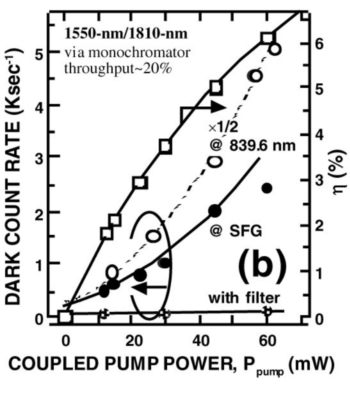

Fig.2. Efficiency and dark count rate as a function of coupled 1810-nm pump power: throughput was ~20 %. The DC rate is reduced to below 100 cps.

InAs Nanowire-channel Field Effect Transistors

Guoqiang Zhang, Kouta Tateno, and Hidetoshi Nakano
Optical Science Laboratory

Recently, nanowires (NWs) have become the center of attention due to the exceptional versatility and promise a wide range of potential applications, from electronics and photonics to biochemistry and medicine [1]. Semiconductor NWs are expected to play an important role as functional device elements in nanoscale electronic devices. InAs NWs are very promising for high-speed device applications due to their high mobility. We have established a reproducible fabrication process for NW field effect transistors (FETs) and the performance of the InAs NW-channel FETs were evaluated [2].

Au colloidal particles were used as the catalyst for the growth of InAs NWs by vapor-liquid-solid mode in a low-pressure (76 Torr) metalorganic vapor phase epitaxy system [3]. The precursors were trimethyl-indium and AsH_3. Transmission electron microscopy measurement indicates that the NWs are wurtzite-structure without stacking faults. The NWs were dispersed on a SiO_2/Si (SiO_2 thickness: 500 nm) substrate and then Ni/Au metals were selectively deposited on the NWs to form electrical contacts after patterning by electron beam lithography. The contacts were annealed at 300 ºC for 30 s by rapid thermal processing. Figure 1 shows a NW-channel FET with a number of electrodes.

Using the underlying heavily doped Si substrate as the gate electrode, we measured the DC characteristics of InAs NW-channel FETs with a semiconductor parameter analyzer at room temperature. Figure 2 shows typical characteristics of I_d-V_d of 2 and 4-terminal measurements. Compared with NW resistance, the contact resistance is very small and the specific contact resistivity is estimated to be 2.0×10^{-7} Ωcm^2. Figure 3 shows typical I_d-V_g characteristics at different drain voltages. The feature that the current increases with the gate voltage indicates that the NW is n-type. The NW-channel FETs show a maximum transconductance (g_m) in the range of 0.24-0.36 μS at V_d of 0.1 V. For FET devices, the normalized transconductance $g^*_m = g_m/w_g$ is an important figure of merit, where w_g is the channel width (in the case of NW channel, the width is the NW diameter). The g^*_m varies in the range of 2.5-3.7 mS/mm at V_d of 0.1 V. Based on the FET properties, the electron concentration (N) and mobility (μ) of the NW segment could be estimated. N and μ are in the range of $2.3\text{-}5.8 \times 10^{17}$ cm^{-3} and $1.29\text{-}1.53 \times 10^3$ cm^{2}V^{-1} s^{-1}, respectively. We are investigating how to further improve the FET properties and fabricate functional quantum devices.

This work was partly supported by JSPS-KAKENHI (16206003, 18310074).

[1] Y. Li, et al., Mater. Today **9(10)** (2006) 18; C. Thelander, et al., ibid. **9(10)** (2006) 28; P. J. Pauzauskie and P. Yang, ibid. **9(10)** (2006) 36.
[2] G. Zhang, et al., ISCS2007, Kyoto, Japan, Oct. 2007, p. 142.
[3] G. Zhang, et al., J. Appl. Phys. **103** (2008) 014301.

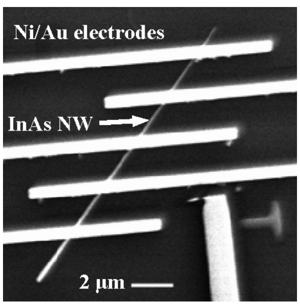

Fig. 1. SEM image of a InAs NWFET.

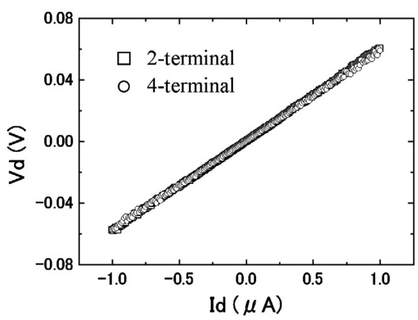

Fig. 2. V_d-I_d characteristics of 2 and 4-terminal measurements.

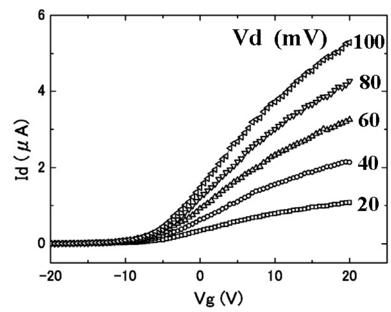

Fig. 3. I_d-V_g characteristics at various drain voltages.

Demonstration of a CEO-locked Frequency Comb at Telecommunications Wavelengths with Low Pulse Energy

Atsushi Ishizawa, Tadashi Nishikawa, and Hidetoshi Nakano
Optical Science Laboratory

The carrier-envelope offset (CEO) is an absolute phase slip between pulses of a mode-locked laser. Recently, progress in the mode-locked laser techniques has made it possible to generate a CEO-locked frequency comb from a mode-locked laser pulse and contains various frequency components in the hundreds of terahertz region which are regularly spaced. The CEO-locked frequency comb can be used as an "optical frequency ruler" with a cesium atomic clock for controlling the spacing. Optical frequency measurement is one of applications of the "ruler". Lasers for applications, such as precision spectroscopy and telecommunications, should be small and have a high repetition rate.

However, CEO frequency detection needs an octave bandwidth spectrum because self-referencing is employed. As a result, a fiber laser needs amplification, which makes it difficult to reduce the size of the laser system. Furthermore, telecommunications and precision spectroscopy applications require a CEO-locked frequency comb with a high repetition rate. The problem in this case is that the pulse energy becomes smaller as the repetition rate increases. We therefore need to achieve CEO locking with a small and high-repetition rate device with low pulse energy.

Our new method employs a tellurite photonic crystal fiber (PCF) for supercontinuum (SC) generation with low pulse energy, and a periodically poled lithium niobate (PPLN) ridge waveguide for efficient second harmonic generation. We found the optimum condition for generating the SC spectrum by changing the polarization of the laser, the PCF length, and the core size. We found that a SC spanning more than an octave can be generated with 80 pJ fiber-coupling pulse energy (Fig. 1). The CEO frequency is measured with an Mach-Zehnder interferometer by combing the second harmonic into a PPLN ridge waveguide with the short wavelength components of the SC light. From the SC shape, we found the optimum wavelength in the 965 nm region in order to observe the CEO frequency. Hartl et al. succeeded in locking the CEO with a 600 pJ fiber coupling pulse energy [1]. We have demonstrated a CEO-locked frequency comb at the telecommunications wavelengths with a 230 pJ fiber coupling pulse energy, which, to the best of our knowledge, is the lowest fiber coupling pulse energy ever achieved (Fig. 2) [2]. Due to the improvement of the coupling efficiency to the PCF, it would be possible to lock the CEO by using a fiber laser oscillator with a low pulse energy.

[1] I. Hartl, et al., Opt. Express **13** (2005) 6490.
[2] A. Ishizawa, et al., Opt. Express **16** (2008) 4706.

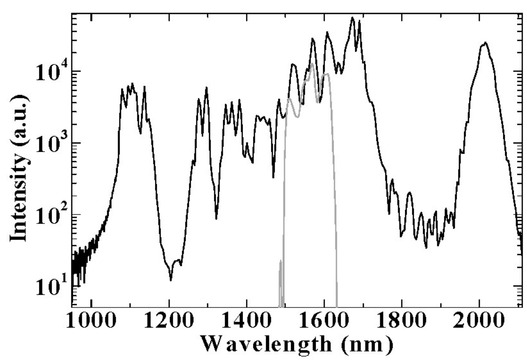

Fig. 1. Spectrum spanning more than an octave (black) and the spectrum of fiber laser (gray).

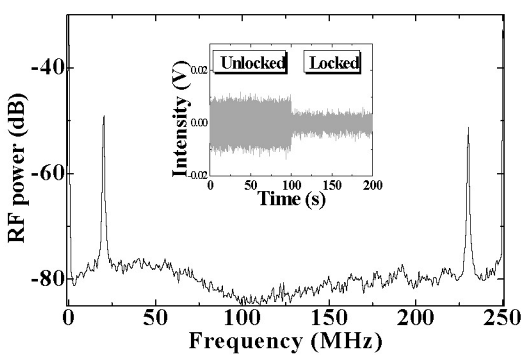

Fig. 2. CEO frequency signal (black) and the phase difference between the CEO signal and a local oscillator (gray).

Ultra High-Q Photonic Crystal Nanocavities Based on Compound Semiconductors

Akihiko Shinya[1], Shinji Matsuo[2], Yosia[1], Takasumi Tanabe[1], Eiichi Kuramochi[1], Takehiko Tawara[1], Kouta Tateno[1], Tomonari Sato[2], Takaaki Kakitsuka[2], and Masaya Notomi[1]
[1]Optical Science Laboratory, [2]NTT Photonics Laboratories

Photonic crystal (PhC) is a promising candidate as a platform to construct devices with dimensions of several wavelengths. A PhC is an artificial structure with light wavelength periodicity that can confine light in an ultra small area of about 0.1 μm^3 with an ultra high Q factor. We have been studying ways of strongly confining light in ultra small areas with the aim of minimizing the light propagation speed and enhancing the light-material interaction by using Si based PhCs. In this report, we adopt new materials, namely InGaAsP and AlGaAsP, to develop a new photonic technology. These materials have certain features that Si does not have, e.g. they exhibit large refractive index modulation owing to optical nonlinearity, and they are expected to be used for PhC based active devices.

Figure 1 shows a scanning electron micrograph of an InGaAsP PhC and transmission spectra of InGaAsP and AlGaAs PhC nanocavities. The PhCs are composed of air holes arranged 420 nm apart in a triangular pattern and they function as a light insulator at a wavelength of around 1.55 μm. The area with no linearly arranged holes is the light waveguide and the area where some holes are shifted few nanometers away from the center of the waveguide functions as a cavity that can confine light [1]. InGaAsP and AlGaAs PhC nanocavities have estimated Q factors of 130,000 and 690,000, respectively. These values are around ten times larger than those previously reported for PhC nanocavities with these materials. They are expected to provide all-optical memories with very low operating power [2] and highly efficient optical-mechanical power converters [3].

This work was supported by the National Institute of Information and Communications Technology (NICT).

[1] E. Kuramochi, et al., Appl. Phys. Lett. **89** (2006) 241124.
[2] T. Tanabe, et al., Opt. Lett. **30** (2005) 2575.
[3] M. Notomi, et al., Phys. Rev. Lett. **97** (2006) 023903.

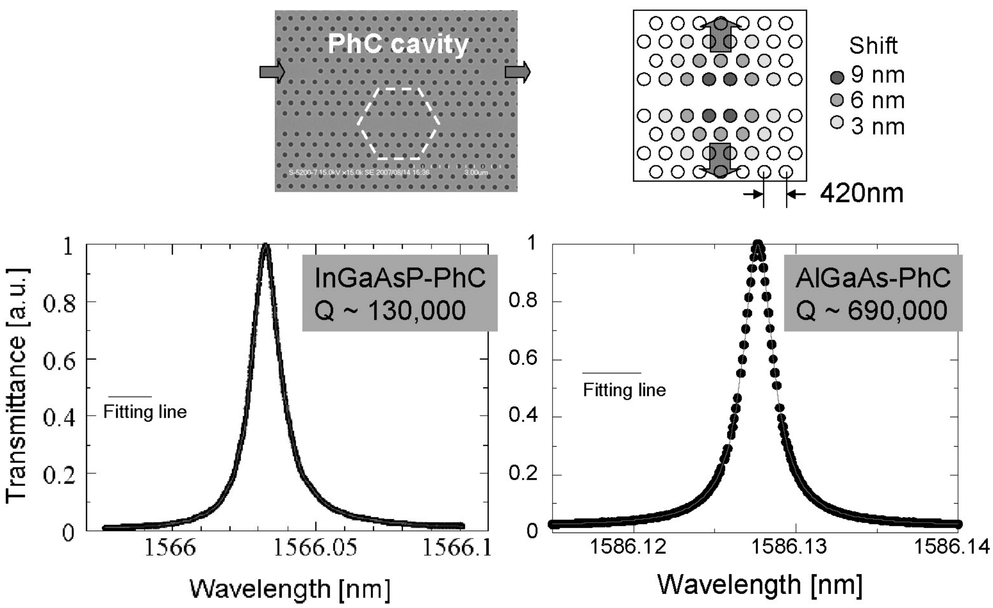

Fig. 1. PhC cavity structure and transmission spectra of InGaAsP and AlGaAs PhCs.

All-optical Bit Memory Based on Photonic Crystal Nanocavity

Akihiko Shinya[1], Shinji Matsuo[2], Yosia[1], Takasumi Tanabe[1], Eiichi Kuramochi[1], Tomonari Sato[2], Takaaki Kakitsuka[2], and Masaya Notomi[1]
[1]Optical Science Laboratory, [2]NTT Photonics Laboratories

We have focused on a resonant tunneling filter on a Si based photonic crystal (PhC) platform where single-mode waveguides (WGs) are effectively coupled with an ultrasmall cavity with a high Q factor. The photon density in the cavity is extremely high owing to its small size and effective coupling with PhC-WGs, and this results in a large optical nonlinearity that enables us to realize all-optical memories with very low operating power [1]. However, it is very difficult to achieve a long memory time for a Si based PhC because of its small optical nonlinearity. In this work, we developed an InGaAsP based PhC nanocavity and realized an all-optical bit memory that can operate at very low power and achieve a long memory time.

Figure 1 shows the bit memory operation of the InGaAsP based PhC nanocavity [2]. The initial state of the memory is OFF and it outputs a low level signal (gray line). When a set pulse with a width of 100 ps is input from the waveguide to write one bit of information, the memory turns ON and outputs a high level signal (black line). The memory remains in the ON state after the set pulse has been applied, which means that the bit information is stored. The longest memory time is 150 ns, which is much longer than that of a Si-PhC memory (2.5 ns). The minimum bias power for the memory operation is 40 μW, which is ten times lower than for a Si-PhC and around 100 times lower than that of a conventional optical memory based on bistable lasers. This technology is expected to eliminate certain photonic device bottlenecks such as the difficulty of dense integration on a chip and the difficulty of achieving low power consumption in all-optical memories.

This work was supported by the National Institute of Information and Communications Technology (NICT).

[1] T. Tanabe, et al., Opt. Lett., **30** (2005) 2575.
[2] A. Shinya, et al., CLEO/QELS2008, San Jose, U.S.A., May 2007.

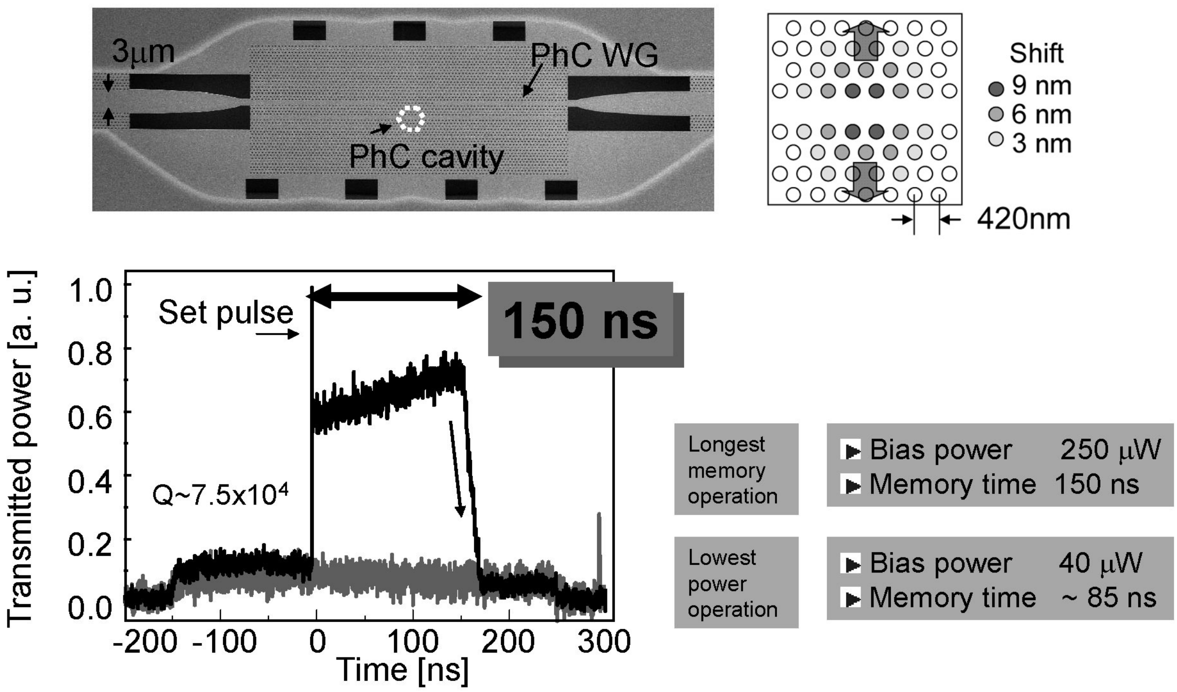

Fig. 1. Bit memory operation of InGaAsP based PhC.

Slow Light Propagation in Large-scale Photonic Crystal Coupled Resonator Waveguides

Eiichi Kuramochi, Takasumi Tanabe, Hideaki Taniyama, and Masaya Notomi
Optical Science Laboratory

A periodic chain of optical resonators (coupled resonator optical waveguide: CROW) is expected to be a promising candidate as a slow light medium [1]. In the last annual report, we mentioned that CROWs composed of ultrahigh quality factor (Q, ~10^6) Si photonic crystal (PhC) resonators [2] could couple more than 60 resonators with a very low propagation loss, which is a unique advantage of the PC-CROW [3]. We also reported the dispersion of the PC-CROWs, which corresponded to a very low group velocity (v_g) [3]. In this work, we greatly improved the passband spectrum of PC-CROW to realize distortion-free short pulse propagation because a short pulse occupies a wide frequency range.

Figure 1 is a schematic of the improved PC-CROW structure. We employed an inline coupling structure to maximize the coupling between the CROW and external waveguides. In addition, the resonator interval was apodized for the same purpose. The passband exhibited close to the ideal low loss, and was wide and flat as shown in Fig. 2. We performed a time domain pulse propagation experiment using a short pulse (FWHM: 16 ps, wavelength: ~1563 nm). The pulse was transmitted through the CROW and was delayed by 35 ps (N=30) and 75 ps (N=60), respectively (N: resonators in CROW), which agreed well with the v_g of 0.0085c (c: light speed in a vacuum) evaluated by dispersion measurement (Fig. 3). The delay was several times larger than the original pulse width, which is unachievable with existing slow light media. Moreover, the pulse distortion and the ringing after-pulse were well suppressed. The results [4] clearly demonstrated the feasibility of a PC-CROW as a slow light medium for high-speed optical communication.

This work was partly supported by CREST of the Japan Science and Technology Agency.

[1] A. Yariv, et al., Opt. Lett. **24** (1999) 711.
[2] E. Kuramochi, et al., Appl. Phys. Lett. **88** (2006) 041112.
[3] E. Kuramochi, et al., CLEO/QELS2007, Baltimore, U.S.A., May 2007, 2.
[4] E. Kuramochi, et al., CLEO/QELS2008, San Jose, U.S.A., May 2008, 3.

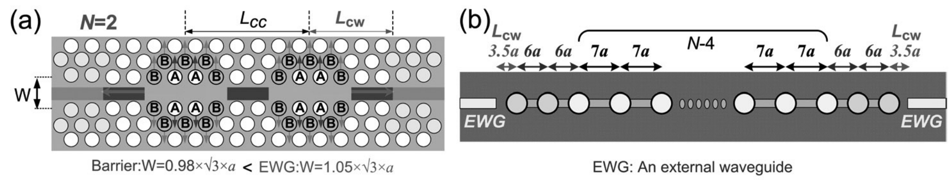

Fig. 1. (a) In-line coupling structure. (L_{cc}: resonator interval; L_{cw}: the distance between the external waveguide and the center of the outermost resonator.) (b) PC-CROW structure studied here. The lattice constant, hole radius, and slab thickness were 420, 110, and 205 nm, respectively. Holes (A/B) were shifted (8/4 nm) away from the line defect.

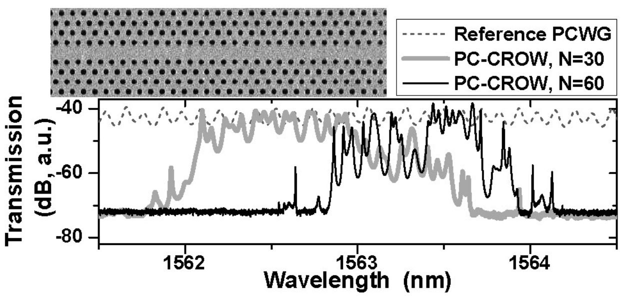

Fig. 2. Transmission spectra of long PC-CROWs (N: number of resonators).

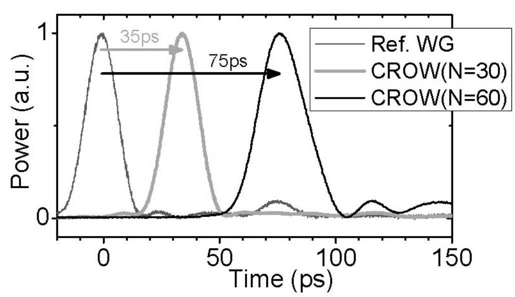

Fig. 3. Time-resolved data of optical pulses after passing through sample recorded with oscilloscope.

Ⅱ. Data

4th NTT-BRL School

The fourth NTT Basic Research Laboratories (BRL) school was held in November 19-22, 2007 at the NTT Atsugi R&D Center. The aim of the NTT BRL school is to foster young researchers in the physics field, as well as to promote the international visibility of NTT BRL. This year the theme was "Recent Status in Quantum Information Technology".

The theam is closely related to the research on quantum information processing that NTT BRL is conducting intensively. Prestigious professors and researchers were invited to the school as lecturers. There were thirty-five participants, mainly Ph. D students, from twelve countries.

On the first day, after the director of NTT BRL had provided an overview of NTT BRL, Prof. Yoshihisa Yamamoto (Stanford University, U.S.A.) presented lectures entitled "Recent Progress in Quantum Information Technology". He also gave lectures on the second and third day that covered related fundamental theories, reviews of experiments and some recent results. Dr. Jaw-Shen Tsai (NEC Nano-electronics Laboratories, Japan) gave a talk on "Superconducting Qubits" on the afternoon of the second day. In this BRL school, there were several lectures by researchers working at NTT BRL. Dr. Toshimasa Fujisawa gave a lecture on "Single-electron Charge and Spin Dynamics in Quantum Dots". Dr. Koichi Semba talked about the "Josephson Circuit QED". Dr. Tetsuya Mukai gave a talk entitled "Persistent Supercurrent Atom Chip". A poster session was held in the evening of the second day, where each student gave a presentation about his/her research at the university. All the students, lecturers, and NTT BRL researchers had a good time exchanging information on current research topics in various fields. On the third and fourth day we provided an overview of NTT BRL. A laboratory tour was conducted so that the students could see the research facilities. Managers of NTT BRL gave talks on recent activities at each laboratory. After that, all the participants attended in NTT BRL Science Plaza 2007, which is an exhibition of recent research achievements and activities. They enjoyed discussions with researchers about on-going research topics indetail.

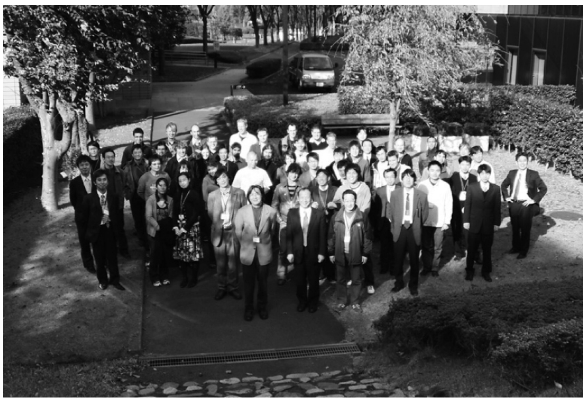

At the farewell party, best poster prizes were awarded to the students who gave noteworthy presentations. The students were able to build friendships and exchange contact addresses. NTT BRL will continue to provide these kinds of occasions to support young researchers and help establish human networks in the fields of physics and applied physics.

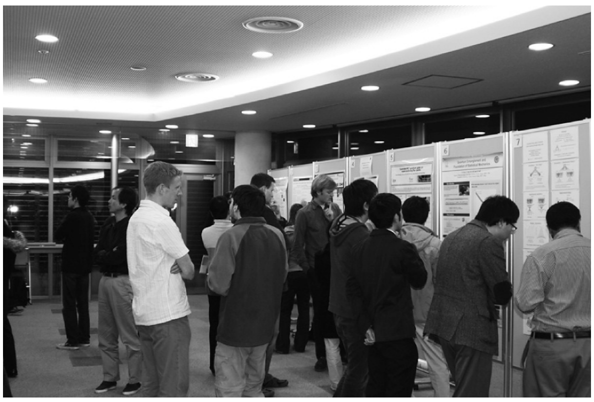

Science Plaza 2007

"Science Plaza 2007", an open-house event of NTT Basic Research Laboratories (BRL), was held at NTT Atsugi R&D Center on Thursday, November 22nd, 2007. Under the banner "Nanoscience Opens Up the Quantum World", Science Plaza aimed to disseminate our latest research accomplishments through various sections of people inside and outside of NTT and to gather diverse opinions.

Following an opening address from the director, Dr. Yumoto, Exective Managers briefly summarized research strategy and exhibited posters. In the afternoon session, two distinguished technical members of NTT BRL, Toshimasa Fujisawa and Akira Fujiwara, gave lectures on "Controlling and detecting single-electron states" and "Control of Single Electrons in Silicon Nanodevices", respectively. Each lecture was well-attended and followed by heated question-and-answer sessions.

As regards the poster exhibits, 34 posters, including four from Photonics Laboratories and Microsystem Integration Laboratories, presented our latest research accomplishments. While explaining the originality and impact—as well as the future prospects—of our research accomplishments, these posters were intensively discussed, and many meaningful opinions were heard. This year’s "Lab Tour"—a guided tour of research facilities at NTT BRL that has been receiving high reputation from visitors over the years—took place at four different labs, each presented five times in total, so that as many people as possible could join the tour. This time we also opened a booth to introduce the NTT R&D recruitment system for job-seeking researchers and students. After all lectures, presentations, and exhibitions, a banquet was held in Center’s dining room, where lively conversation among participants deepened their amity.

More than 200 people from research institutes, universities, and general industries, as well as from NTT Group, attended Science Plaza 2007. Thanks to the efforts of all participants, the conference ended on a high note. We would thus like sincerely to express our gratitude to all of the participants.

Award Winners' List (Fiscal 2007)

Photonic & Electromagnetic Crystal Structures (PECS) VII First Place Poster Award	E. Kuramochi	Low Loss Long Coupled Resonator Optical Waveguides Realized Using Ultrahigh-Q Photonic Crystal Resonators	Apr. 10, 2007
14th Semiconducting and Insulating Materials Conferences (SIMC XIV) Young Scientist Award	Y. Taniyasu	For Outstanding Contributions in Developing and Implementing Aluminum Nitride Deep-ultraviolet Light-emitting Diodes	May 17, 2007
The Laser Society of Japan The 31st Original Paper Award	T. Tanabe A. Shinya S. Kawanishi M. Notomi	All-optical Switching and 5-GHz RZ (Return to Zero) Optical Pulse Train Modulation Using Silicon Photonic Crystal Cavities	May 31, 2007
12th Optoelectronics and Communication Conference IEEE/LEOS Japan Chapter Student Award	T. Yamaguchi	Fabrication and Optical Properties of Hybrid-type Pillar Microcavity	July 11, 2007
SSDM Young Researcher Award	A. Nishikawa	High Critical Electric Field Exceeding 8 MV/cm Measured Using AlGaN p-i-n Vertical Conducting Diode on n-SiC Substrate	Sep. 19, 2007
SSDM Paper Award	T. Sogawa H. Gotoh Y. Hirayama T. Saku P. V. Santos K. H. Ploog	Optical Properties of Dynamically-modulated Dots and Wires Formed by Surface Acoustic Waves	Sep. 19, 2007
The 6th Annual Scientific American 50	T. Tanabe	Storing Photons in a Photonic Crystal	Nov. 30, 2007
Gordon Research Conferences: Magnesium in Biochemical Processes & Medicine Best Poster Presentation Award	K. Torimitsu Y. Shinozaki Y. Furukawa	Magnesium Effect on Brain Neural Development	Mar. 13, 2008
The Japan Society for the Advancement of Invention Special Award	A. Shimada （TESTRONICS CO., LTD）	Extensometers for Fine Wires	Mar. 18, 2008
Young Scientist Award of the Physical Society of Japan	N. Kumada	Electron Spins in Bilayer Quantum Hall Systems Investigated by Nuclear Spin Measurement	Mar. 23, 2008

In-house Award Winners' List (Fiscal 2007)

NTT R&D Award	A. Fujiwara K. Nishiguchi Y. Ono K. Yamazaki	Manipulation and Detection of a Single Electron Using Silicon Nano MOSFET	Dec. 13, 2007
NTT R&D Award	T. Tanabe M. Notomi E. Kuramochi A. Shinya H. Taniyama	Slowing Down Light to One 50 Thousandth of Its Speed	Dec. 13, 2007
Award for Achievements by Director of Basic Research Laboratories	S. Saito J. Johansson K. Kakuyanagi T. Meno H. Nakano K. Semba	Quantum Electrodynamics Using Superconducting Quantum Circuits	Mar. 17, 2008
Award for Achievements by Director of Basic Research Laboratories	K. Suzuki K. Kanisawa	Imaging of Electron Wave Interference by Scanning Tunneling Spectroscopy on Cleaved Semiconductor Heterostructure Surfaces	Mar. 17, 2008
Award for Achievements by Director of Basic Research Laboratories	A. Yokoo H. Namatsu	Nanoelectrode Lithography	Mar. 17, 2008
Award for Excellent Papers by Director of Basic Research Laboratories	T. Mukai	"Persistent Supercurrent Atom Chip", Phys. Rev. Lett. **98** (2007) 260407.	Mar. 17, 2008
Special Award by Director of Basic Research Laboratories	M. Yamaguchi K. Suzuki H. Ito H. Ueshima Y. Ono	Substantial Improvement in the Recycling Rate of Liquid Helium by the Web-Based System	Mar. 17, 2008
Special Award by Director of Basic Research Laboratories	S. Sasaki	Electron Beam Exposure System at NTT Basic Research Laboratories	Mar. 17, 2008

List of Visitors' Talks (Fiscal 2007)

I. Materials Science

Date	Speaker	Affiliation Title
Apr. 24	Dr. Chandra S. Ramanujan	University of Oxford, U.K. "The NTT Oxford Collaboration: Studying Biological Systems Using Atomic Force Microscopy"
May 8	Dr. Simon Koblar	University of Adelaide, Australia "Stem Cell Therapy for Improvement in Stroke Outcome"
May 18	Prof. Robert Vink	University of Adelaide, Australia "Role of Magnesium in Brain Damage and the Receptor Relation"
May 29	Dr. Hideyuki Maki	Keio University "Carrier Injection Control and Bandgap Control of Carbon Nanotubes"
June 1	Prof. Erhard Kohn	University of Ulm, Germany "Electronic Diamond Surface Characteristics"
June 14	Prof. Shingo Tsukada	The Graduate University of Japan Traditional Medicine and Science "Monitoring of Biological Information Using Meridian Related Impedance Measurement"
Sep. 18	Dr. Achillefs Kapanidis	University of Oxford, U.K. "Studying Biomachines and Biosensors Using Single-molecule Fluorescence"
Oct. 24	Prof. David J. Rogers	University of Technology of Troyes, France "Use of ZnO Thin Films as Sacrificial Templates for MOVPE and Chemical Lift-off of GaN"
Oct. 25	Dr. Kimiko Yamamoto	The University of Tokyo "Regulation of Circulatory Function by Vascular Endothelial P2X4 Receptor"
Nov. 16	Prof. Jun Suda	Kyoto University "Growth of High-quality AlN on SiC (0001) by Step-height Control and Growth of Novel-polytype AlN on SiC with Non-polar Crystal Faces"
Dec. 18	Prof. Seiji Samukawa	Tohoku University "Damage-free Neutral Particle Beams for Nano-device Fabrication"

II. Physical Science

Date	Speaker	Affiliation Title
Apr. 9	Mr. Takahiro Morimoto	Chiba University "Non-local Transport Measurement Approach to 0.7 Structure in Quantized Conductance"
July 25	Prof. Gerald Bastard	National Center for Scientific Research, France "Quantum Cascade Lasers in a Magnetic Field"
July 26	Dr. Kris Helmerson	National Institute of Standards and Technology, U.S.A. "Vortices and Persistent Currents in Bose-Einstein Condensates"
Aug. 21	Prof. Robert H. Blick	University of Wisconsin-Madison, U.S.A. "Nano-electromechanical Systems"
Aug. 22	Prof. Hongqi Xu	Lund University, Sweden "Symmetry, Spin Hall Effect and Zitterbewegung in Electron Waveguides with Spin-orbit Interaction"
Oct. 9	Prof. Tetsuo Ogawa	Osaka University "Mechanism of Optical Gain Production in the Presence of Carrier-carrier Interaction in Quantum Wires: Screened Hartree-Fock Approximation and Dynamical Mean-field Approximation"
Oct. 22	Dr. Henning Riechert	Qimonda AG, Germany "GaN and Si Nanowires: Growth Studies and Transistor Results"
Oct. 29	Prof. Alexey Ustinov	University of Erlangen-Nuremberg, Germany "Temperature-induced Decoherence in Josephson Phase Qubits"
Nov. 5	Prof. Klaus H. Ploog	Paul Drude Institute, Germany "III-Nitrides Seem to be Good for Everything"
Nov. 2	Prof. Hong Zhang	Sichuan University, China "Oxygen Adsorption on the Ir(111): A First Principle Study"
Nov. 8	Dr. William D. Oliver	Massachusetts Institute of Technology, U.S.A. "Mach-Zehnder Interferometry and Microwave-induced Cooling in Persistent-current Qubits"
Nov. 8	Dr. Tristan Meunier	Delft University of Technology, the Netherland "Relaxation and Coherent Manipulation in Spin Qubits"
Nov. 22	Mr. Erik Lucero	University of California, Santa Barbara, U.S.A. "Recent Advances in Josephson Phase Qubits: High Fidelity Gates, Quantum Memory, and Bell Violation"

Dec. 5	Dr. Hiroaki Koga	National Institute for Materials Science, Japan Society for the Promotion of Science "First-principles Study on Elementary Processes in the Growth of Thin Films and Nano-structures"
Dec. 13	Dr. Tiefu Li	NEC-RIKEN, Tsinghua University, China "Making Use of Suspended Metal Nanostructures"
Dec. 18	Prof. Vladimir Antonov	Royal Holloway, University of London, U.K. "Toward Passive Terahertz Imaging"
Dec. 25	Mr. Zhongchang Wang	The University of Tokyo "First-principles Study toward the Understanding of Ag_2S Atomic Switch"
Jan. 30	Dr. Masafumi Jo	Hokkaido University "Towards the Realization of Superconductor-based Light Emitting Diodes"
Feb. 25	Dr. Alberto Morpurgo	Delft University of Technology, the Netherland "Quantum Transport through Graphene Single- and Double-layers"
March 17	Mr. Hiroki Morishita	Keio University "Electrically Detected Electron and Nuclear Spin Resonance of Phosphorus in Silicon"

III. Optical Science

Date	Speaker	Affiliation Title
Apr. 6	Prof. Robert M. Westervelt	Harvard University, U.S.A. "Integrated Circuit / Microfluidic Chips for the Manipulation of Biological Cells"
May 15	Mr. Hong C. Nguyen	University of Sydney, Australia "Enhanced Kerr Nonlinearity in As_2Se_3 Chalcogenide Fibre Tapers with Sub-wavelength Diameter"
May 31	Prof. Kazuki Koshino	Tokyo Medical and Dental University, JST PRESTO "Use of the Classical Input for Solving the Two-photon Nonlinear Dynamics"
June 22	Dr. Qiang Zhang	Stanford University, U.S.A. "Experimental Quantum Teleportation of a Two-qubit Composite System"
June 27	Prof. Norio Kawakami	Kyoto University "Orbital Kondo Effect in Quantum Dot Systems - Application of the Exact Solution -"

Aug. 3	Prof. Shmuel Gurvitz	Weizman Institute, Israel "Lapse of Transmission Phase and Electron Molecules in Quantum Dots"
Aug. 8	Dr. Tatsuya Fujii	The University of Tokyo "Formula of Shot Noise in a Mesoscopic Conductor Based on Keldysh Formalism"
Aug. 22	Prof. Shmuel Gurvitz	Weizman Institute, Israel "Quantum Mechanical Approach to Decoherence and Relaxation Generated by Fluctuating Environment"
Sep. 10	Prof. Xin-Qi Li	Chinese Academy of Science, China "Particle-number-resolved Master Equation to Quantum Transport, Quantum Measurement, and Quantum Control"
Oct. 22	Dr. Paulo V. Santos	Paul Drude Institute, Germany "Control of Photons and Excitons Using Surface Acoustic Waves"
Nov. 9	Mr. Tomohiro Amemiya	The University of Tokyo "Ferromagnet-semiconductor Composite Devices for Waveguide Isolators"
Nov. 26	Mr. Odilon D. D. Couto Jr.	Paul Drude Institute, Germany "Spin Transport and Relaxation in (110) GaAs Quantum Wells Using Surface Acoustic Waves"
Nov. 30	Dr. Andrew Shields	Toshiba Research Europe Ltd., Cambridge Research Laboratory, U.K. "Single Photon Technology for Quantum Information Applications"
Jan. 9	Dr. Jean Benoit Heroux	The University of Tokyo "Characterization of GaMnAs by Time-resolved Mid-infrared Transmittance and THz Emission"
Jan. 29	Dr. Renato Renner	Swiss Federal Institute of Technology, Switzerland "Symmetries and Cryptography"
Feb. 27	Mr. Tony Pisano	NP Photonics, U.S.A. "Recent Status in Optical Fiber Lasers in Telecom-band"
March 17	Prof. Takaaki Mukai	Osaka City University "Modulation Characteristics in Semiconductor Lasers with Fiber Bragg Gratings"

Research Activities in Basic Research Laboratories in 2007

The numbers of papers published in international journals, presentations at international conferences and applied patents in year 2007 amounted to 140, 269, and 48, respectively. The numbers for each research area are as follows;

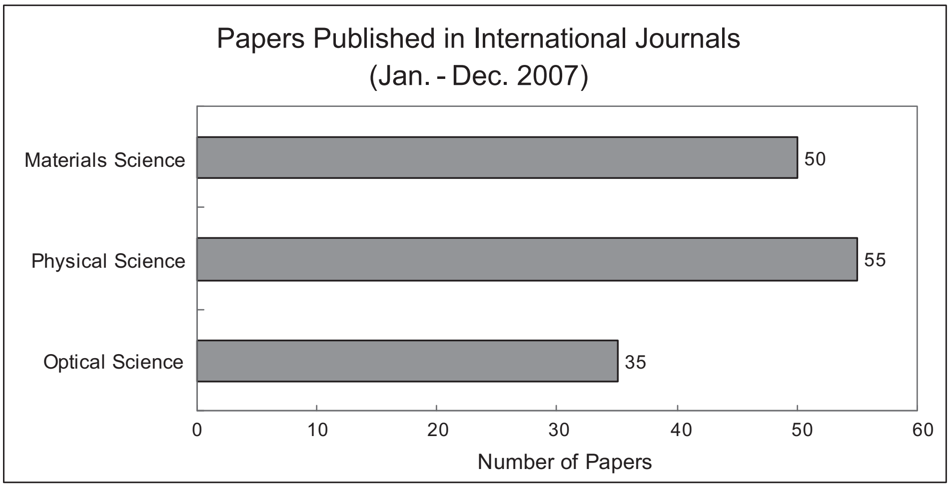

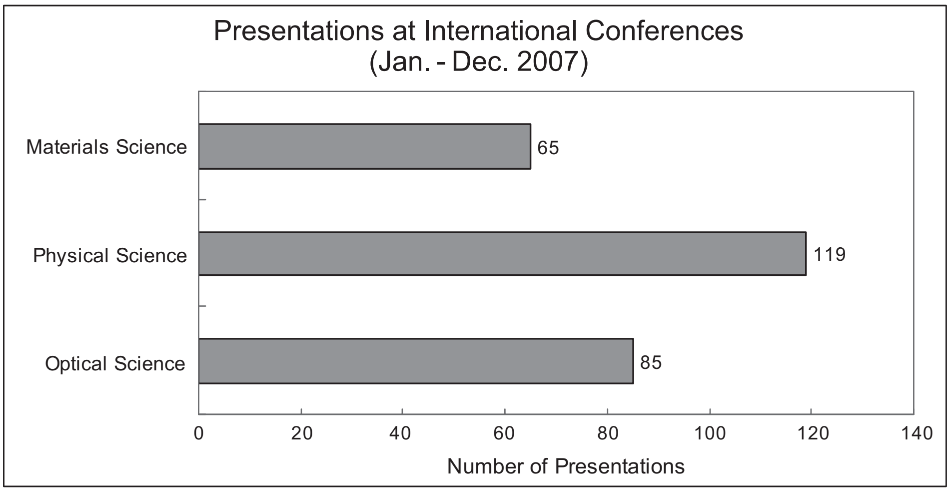

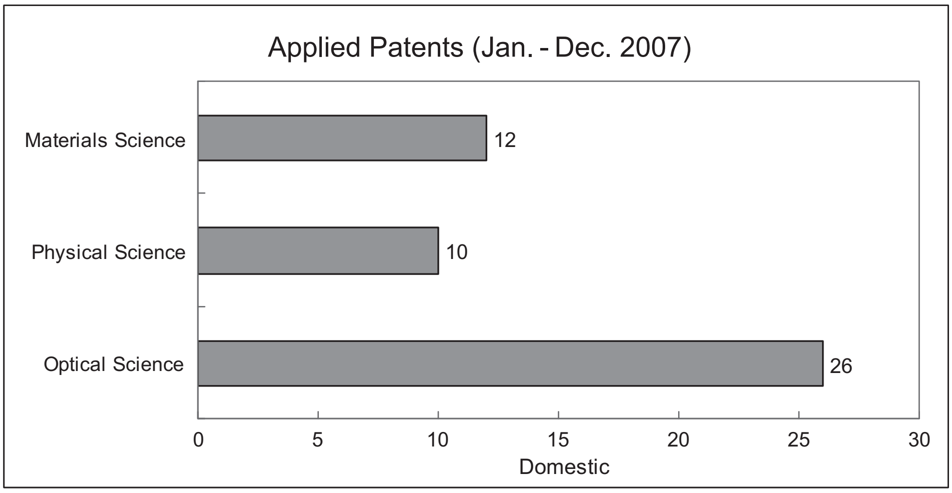

The numbers of research papers published in the major journals are shown below.

Journals	(IF2006*)	Numbers
Applied Physics Letters	3.977	26
Chemical Communications	4.521	1
IEEE Electron Device Letters	2.716	2
IEEE Transactions on Electron Devices	2.052	2
Japanese Journal of Applied Physics	1.222	19
Journal of Applied Physics	2.316	3
Journal of Crystal Growth	1.809	12
Journal of the American Chemical Society	7.696	1
Nano Letters	9.960	2
Nature	26.681	1
Nature Photonics	-	2
Nature Physics	12.040	1
Neuroscience Research	1.953	2
New Journal of Physics	3.754	3
Optics Express	4.009	7
Physica E-Low-Dimensional Systems & Nanostructures	1.084	4
Physical Review B	3.107	9
Physical Review Letters	7.072	9

*IF2006 : Impact Factor 2006 (Journal Citation Reports,2006)

The average IF2006 for all research papers from NTT Basic Research Laboratories is 3.23.

The numbers of presentations in the major conferences are shown below.

Conferences	Numbers
International Conference on Nanoelectronics, Nanostructures and Carrier Interactions	27
International Conference on Electronic Properties of Two-dimensional Systems and Modulated Semiconductor Structures	24
The 34th International Symposium on Compound Semiconductors	17
2007 International Conference on Solid State Devices and Materials	13
9th International Conference on Atomically Controlled Surfaces, Interfaces and Nanostructures	10
Frontiers in Nanoscale Science and Technology Workshop	9
2nd International Symposium on Nanometer-Scale Quantum Physics	7
The American Physical Society	7
The Conference on Lasers and Electro-Optics and the Quantum Electronics and Laser Science Conference	7
17th International Vacuum Congress, 13th International Conference on Surface Science and International Conference on Nano Science and Technology	7
International Symposium on Advanced Nanodevices and Nanotechnology	7
Fourth International Conference on Molecular Electronics and Bioelectronics	4
The 1st Conference of New Diamond and Nano Carbons	4
Silicon Nanoelectronics Workshop	4
The 3rd Workshop of the UK-Japan Bionanotechnology Collaboration	4
15th International Conference on Nonequilibrium Carrier Dynamics in Semiconductors	4
Asian Conference on Quantum Information Science	4
20th International Symposium on Superconductivity	4

List of Invited Talks at International Conferences (2007)

I. Materials Science Laboratory

(1) H. Omi, T. Kawamura, Y. Kobayashi, S. Fujikawa, Y. Tsusaka, K. Kagoshima, and J. Matsui, "Strain Analysis of Semiconductor Nanoscale Thin Films by Grazing Incidence X-ray Diffraction", Symposium on Surface and Nano Science 2007, Appi, Japan (Jan. 2007).

(2) K. Furukawa, "FRET Observation Using Lipid-flow Chip", International Mini-symposium of Surface Forces, Matsushima, Japan (Mar. 2007).

(3) K. Kumakura, A. Nisikawa, and T. Makimoto, "Nitride-based Heterojunction Bipolar Transistors for High-power and High-temperature Electronics", The 4th International Symposium on Ubiquitous Knowledge Network Environment, Sapporo, Japan (Mar. 2007).

(4) Y. Taniyasu, M. Kasu, and T. Makimoto, "AlN p-n Junction UV-LEDs", The 3rd Asia-Pacific Workshop on Widegap Semiconductors, Jeonju, Korea (Mar. 2007).

(5) M. Kasu, K. Ueda, A. Tellaire, and T. Makimoto, "Diamond RF Power Transistors", 2nd International Industrial Diamond Conference, Rome, Italy (Apr. 2007).

(6) K. Torimitsu, "Functional Analysis of Neurons and Receptor Proteins for Device Application", 1st International Symposium on Nanomedicine from Basic to Applications, Okazaki, Japan (Apr. 2007).

(7) Y. Taniyasu, M. Kasu, and T. Makimoto, "AlN Deep-ultraviolet Light-emitting Diodes", 14th Semiconducting and Insulating Materials Conference, Arkansas, U.S.A. (May 2007).

(8) Y. Taniyasu, M. Kasu, and T. Makimoto, "AlN Deep-UV Light-emitting Diodes by MOVPE", 12th Euroepan Workshop on Metalorganic Vapour Phase Epitaxy, Slovakia, Bratislava (Jun. 2007).

(9) K. Ueda and M. Kasu, "Diamond Transistors for RF Power Amplifiers", IEEE MTT-S International Microwave Symposium, Hawaii, U.S.A. (Jun. 2007).

(10) K. Ajito, "Teahertz and Raman Spectoroscopy for Biological Applications", 2007 SURA Terahertz Applications Symposium, Washington, DC, U.S.A. (Jun. 2007).

(11) H. Omi, "Scaling and Universality of Morphological Transition at the SiO_2/Si(001) Interface", Gordon Research Conference on Thin Film and Crystal Growth Mechanisms, South Hadley, U.S.A. (Jun. 2007).

(12) K. Ajito, "Terahetz and Raman Biospectroscopy", 3rd Asian and Pacific Rim Symposium on Biophotonics, Cairns, Australia (Jul. 2007).

(13) Y. Taniyasu, M. Kasu, and T. Makimoto, "AlN Deep-UV Light-emitting Diodes", 18th European Conference on Diamond, Diamond-Like Materials, Carbon Nanotubes, and Nitrides, Berlin, Germany (Sep. 2007).

(14) K. Torimitsu, "Protein Nanobio Device and its Configuration", 33rd International Conference on Micro- and Nano- Engineering, Copenhagen, Denmark (Sep. 2007).

(15) M. Kasu, K. Ueda, H. Kageshima, and Y. Taniyasu, "Diamond RF FETs and Other Applications in Electronics", The 34th International Symposium on Compound Semiconductors, Kyoto, Japan (Oct. 2007).

(16) K. Torimitsu, "Receptor Protein Analysis and Neurological Functions for Nanobio Interface", The 2nd Neural Stem Cells & Frontier Technologies for Brain Repair Workshop combined with The 2nd Australian Workshop on Computational Neuroscience, Adelaide, Australia (Dec. 2007).

II. Physical Science Laboratory

(1) K. Semba, "Vacuum Rabi Oscillations Observed in a Flux Qubit LC-oscillator System", American Physical Society March Meeting, Denver, U.S.A. (Mar. 2007).

(2) K. Muraki, N. Kumada, and Y. Hirayama, "Low Frequency Spin Dynamics in a Quantum Hall Canted Antiferromagnet", American Physical Society March Meeting, Denver, U.S.A. (Mar. 2007).

(3) K. Kanisawa, "Imaging Donor States in Semiconductor Structures", Frontiers in Nanoscale Science and Technology Workshop (FNST2007), Tokyo, Japan (Mar. 2007).

(4) G. Shinkai, T. Hayashi, Y. Hirayama, and T. Fujisawa, "Electrostatic Coupling Between Two Double-quantum Dots: Toward Two-qubit Manipulation", Quantum Information Processing on Quantum Dots, Windermere, U.K. (Apr. 2007).

(5) H. Kageshima, M. Uematsu, T. Akiyama, and T. Ito, "Microscopic Mechanism of Silicon Thermal Oxidation Process", ECS Meeting, 2007 Spring, Chicago, U.S.A. (May 2007).

(6) H. Tamura, M. Yamaguchi, S. Nomura, T. Akazaki, T. Maruyama, S. Miyashita, and Y. Hirayama, "Simultaneous Measurement of Photoluminescence and Capacitance Spectra in a GaAs Quantum Well", Optical Properties of Low-Dimensional Systems, Ottawa, Canada (May 2007).

(7) K. Nishiguchi, Y. Ono, A. Fujiwara, H. Inokawa, and Y. Takahashi, "Room-temperature-operating Single-electron Devices Using Silicon Nanowire MOSFET", 2007 Asia-Pacific Workshop on Fundamentals and Applications of Advanced Semiconductor Devices, Jeonju, Korea (Jun. 2007).

(8) N. Kumada, K. Muraki, and Y. Hirayama, "NMR Study of a Canted Antiferromagnet in a Bilayer Quantum Hall System", International Conference on Electronic Properties of Two-dimensional Systems, Geneva, Italy (Jul. 2007).

(9) I. Suemune, H. Kumano, Y. Hayashi, K. Tanaka, T. Akazaki, M. Jo, and Y. Idutsu, "Controlled Photon Generation Processes from Semiconductor Quantum Dots and their Applications", The 34th International Symposium on Compound Semiconductors, Gwangju, Korea (Sep. 2007).

(10) C. Hufnagel, T. Mukai, and F. Shimizu, "Manipulation of Cold Atoms on a Superconductive Atom Chip", BOSE-EINSTEIN CONDENSATION 2007- Frontiers in Quantum Gases -, Sant Feliu de Guixols (Costa Brava), Spain (Sep. 2007).

(11) Y. Ono, M. Khalafalla, K. Nishiguchi, K. Takashina, A. Fujiwara, S. Horiguchi, H. Inokawa, and Y. Takahashi, "Charge Transport in Boron-doped Nano MOSFETs: Towards Single-dopant Electronics", Fifth International Symposium on Control of Semiconductor Interfaces, Tokyo, Japan (Nov. 2007).

(12) I. Suemune, H. Kumano, Y. Hayashi, K. Tanaka, T. Akazaki, M. Jo, and Y. Idutsu, "Photon Generation Processes from Semiconductor Quantum Dots: Their Control and Applications", 8th Chitose International Forum, Chitose, Japan (Nov. 2007).

(13) H. Yamaguchi, I. Mahboob, H. Okamoto, and K. Onomitsu, "Micromechanical Devices for Characterizing Electron Behavior in Quantum Systems", International Symposium on Advanced Nanodevices and Nanotechnology, Hawaii, U.S.A. (Dec. 2007).

(14) K. Muraki, "Nuclear Spin Manipulation in Semiconductor Nanostructures", Microelectronics, MEMS, and Nanotechnology 2007, Canberra, Australia (Dec. 2007).

(15) I. Suemune, H. Kumano, Y. Hayashi, K. Tanaka, T. Akazaki, M. Jo, and Y. Idutsu, "Possibility of Semiconductor-based Single Photon Sources for Quantum Information Networks", International Conference on Microwaves and Optoelectronics, Aurangabad, India (Dec. 2007).

III. Optical Science Laboratory

(1) M. Notomi, "Adiabatic Wavelenth Conversion and Optomechanical Energy Conversion in Photonic Crystal Cavities", Photonics West, San Jose, U.S.A. (Jan. 2007).

(2) H. Nakano, K. Oguri, Y. Okano, and T. Nishikawa, "Femtosecond Laser-induced Ablation Processes Observed by Picosecond-time-resolved XAFS Using Femtosecond Laser-produced Plasma Soft X-ray Pulses", The 2nd Canada-Japan SRO-COAST Symposium on Ultrafast Intense Laser Science, Quebec, Canada (Mar. 2007).

(3) M. Notomi, A. Shinya, T. Tanabe, E. Kuramochi, and H. Taniyama, "Photonic-Crystal-Based Chip-Scale Optical Integration", Optical Fiber Communication Conference/National Fiber Optic Engineers Conference, Anaheim, U.S.A. (Mar. 2007).

(4) M. Notomi, T. Tanabe, E. Kuramochi, H. Taniyama, and A. Shinya, "All-Optical Control of Light in Ulrahigh-Q Photonic Crystal Cavities", International Symposium on Photonic and Electrmagnetic Crystal Structures VII, Montrey, U.S.A. (Apr. 2007).

(5) M. Notomi, T. Tanabe, E. Kuramochi, A. Shinya, and H. Taniyama, "All-Optical Control of Light in Ulrahigh-Q Photonic Crystal Cavities", The European Conference on Lasers and Electro-Optics and the International Quantum Electronics Conference, Munich, Germany (Jun. 2007).

(6) H. Nakano, "Spatiotemporally Resolved XAFS Measurement using Femtosecond Laser Plasma Soft X-ray", 3rd Asian Symposium of Intense Laser Science, Cameron Highlands, Malaysia (Jul. 2007).

(7) M. Notomi, T. Tanabe, E. Kuramochi, H. Taniyama, and A. Shinya, "Dynamic Control of Light in High-Q Photonic Crystal Nanoavities", OSA Topical Meeting of Nonlinear Optics, Cona, U.S.A. (Jul. 2007).

(8) M. Yamashita, "Metal-insulator Transition in the Three-dimensional Hubbard Model with Harmonic Confinement", 16th International Laser Physics Workshop, Leon, Mexico (Aug. 2007).

(9) T. Honjo, H. Takesue, H. Kamada, K. Nishida, O. Tadanaga, M. Asobe, and K. Inoue, "Long-distance Distribution of Time-bin Entangled Photon Pairs over 100 km Using Frequency Up-conversion Detectors", 16th International Laser Physics Workshop, Leon, Mexico (Aug. 2007).

(10) M. Notomi, T. Tanabe, E. Kuramochi, A. Shinya, and H. Taniyama, "Photonic Crystal Nanocavities: Slow Light, All-optical Processing, Wavelength Conversion, Optical MEMS", Group IV Photonics 2007, Tokyo, Japan (Sep. 2007).

(11) Y. Tokura, "Latest Achievement in QKD Experiments at NTT", Updating Quantum Cryptography 2007, Tokyo, Japan (Oct. 2007).

(12) H. Takesue, "R&D of Quantum Relay Technology at NTT", Updating Quantum Cryptography 2007, Tokyo, Japan (Oct. 2007).

(13) M. Notomi, "Photonic Quasicrystal Distributed Feedback Lasers", The First International Congress on Advanced Electromagnetic Materials for Microwaves and Optics, Rome, Italy (Oct. 2007).

(14) M. Notomi, "Control of Light in Photonic Crystals", Korea Photonics Conference, Jeju, Korea (Nov. 2007).

(15) Y. Tokura, "Single Spin Manipulation by Electric Field in a Quantum Dot", 2nd International Workshop on Materials Science and Nano-Engineering, Awaji, Japan (Dec. 2007).

(16) M. Notomi, T. Tanabe, E. Kuramochi, H. Taniyama, and A. Shinya, "Dynamic Control of Light by Photonic-Crystal Nanocavities", International Symposium on Advanced Nanodevices and Nanotechnology Waikoloa, Hawaii, U.S.A. (Dec. 2007).

(17) M. Notomi, T. Tanabe, E. Kuramochi, H. Taniyama, and A. Shinya, "Dynamic Control of Light by Photonic-Crystal Nanocavities", The 5th International Conference on Advanced Materials and Devices, Jeju, Korea (Dec. 2007).

NTT Basic Research Laboratories
3-1 Morinosato Wakamiya, Atsugi
Kanagawa, 243-0198 Japan
URL: http://www.brl.ntt.co.jp/